

1
2
3 **Interpretation of Particle Number Size**
4 **Distributions Measured across an Urban**
5 **Area during the FASTER Campaign**
6
7
8

9 **Roy M. Harrison^{1*†}, David C.S. Beddows¹**
10 **Mohammed S. Alam¹, Ajit Singh¹, James Brean¹,**
11 **Ruixin Xu¹, Simone Kotthaus² and Sue Grimmond²**
12

13
14 **¹Division of Environmental Health and Risk Management,**
15 **School of Geography, Earth and Environmental Sciences**
16 **University of Birmingham**
17 **Edgbaston, Birmingham B15 2TT**
18 **United Kingdom**
19

20 **²Department of Meteorology**
21 **University of Reading, Reading RG6 6BB**
22 **United Kingdom**
23

* To whom correspondence should be addressed.
Tele: +44 121 414 3494; Fax: +44 121 414 3709; Email: r.m.harrison@bham.ac.uk

†Also at: Department of Environmental Sciences / Center of Excellence in Environmental Studies, King Abdulaziz University, PO Box 80203, Jeddah, 21589, Saudi Arabia

24 **ABSTRACT**

25 Particle number size distributions have been measured simultaneously by Scanning Mobility
26 Particle Sizers (SMPS) at five sites in Central London for a one month campaign in January –
27 February 2017. These measurements were accompanied by condensation particle counters (CPC)
28 to measure total particle number count at four of the sites and aethalometers measuring Black
29 Carbon (BC) at five sites. The spatial distribution and inter-relationships of the particle size
30 distribution and SMPS total number counts with CPC total number counts and Black Carbon
31 measurements have been analysed in detail as well as variations in the size distributions. One site
32 (Marylebone Road) was in a heavily-trafficked street canyon, one site (Westminster University)
33 was on a rooftop adjacent to the Marylebone Road sampler, a further sampler was located at
34 Regent's University within a major park to the north of Marylebone Road. A fourth sampler was
35 located nearby at 160 m above ground level on the BT tower and a fifth sampler was located 4 km
36 to the west of the main sampling region at North Kensington. Consistent with earlier studies it was
37 found that the mode in the size distribution had shifted to smaller sizes at the Regent's University
38 (park) site, the mean particle shrinkage rate being 0.04 nm s^{-1} with slightly lower values at low wind
39 speeds and some larger values at higher wind speeds. There was evidence of complete evaporation
40 of the semi-volatile nucleation mode under certain conditions at the elevated BT Tower site.
41 Whereas SMPS total count and Black Carbon showed typical traffic-dominated diurnal profiles, the
42 CPC count data typically peaked during nighttime as did CPC/SMPS and CPC/BC ratios. This is
43 thought to be due to the presence of high concentrations of small particles (2.5 – 15 nm diameter)
44 probably arising from condensational growth from traffic emissions during the cooler nighttime
45 conditions. Such behaviour was most marked at the Regent's University and Westminster
46 University sites and less so at Marylebone Road, while at the elevated BT Tower site the ratio of
47 particle number (CPC) to Black Carbon peaked during the morning rush hour and not at nighttime,
48 unlike the other sites. An elevation in nucleation mode particles associated with winds from the

49 West and WSW sector was concluded to result from emissions from London Heathrow Airport,
50 despite a distance of 22 km from the Central London sites.

51

52 **1. INTRODUCTION**

53 The adverse health consequences of air polluted by particulate matter are now well recognised
54 (WHO, 2006). While the main focus has been on the public health impact of exposure to fine
55 particulate matter measured by mass (PM_{2.5}), there has also been concern over the possible
56 contribution of ultrafine particles of less than 100 nm diameter to adverse health outcomes. While
57 such particles contribute little to the total mass of particles in the atmosphere, they dominate particle
58 number (Harrison et al., 2000) and authoritative reviews have concluded that although evidence is
59 currently highly incomplete, they may contribute to the toxic hazard associated with ambient
60 particulate matter (HEI, 2013; WHO, 2013). There have also been suggestions that particle surface
61 area plays a major role in health impacts and this resides largely in the accumulation mode which is
62 typically centred around 100-200 nm diameter (Harrison et al., 2000). Consequently, there is a
63 strong interest from a health perspective in sub-micrometre particles and there are many reports of
64 their concentrations and size distributions within the atmosphere (Asmi et al., 2011; Kumar et al.,
65 2010; 2014).

66
67 In addition to concerns over human health, there are other reasons for the study of the size
68 distribution of airborne particles. Not only does this strongly influence their location and efficiency
69 of deposition in the human lung, the particle size distribution can also be a strong indicator of
70 particle source, with there being some clear differences between the modal diameter of particles
71 arising from different sources (Vu et al., 2015a). The clearest distinction is between particles
72 arising from combustion and other high temperature sources, which tend to be predominantly very
73 small, and particles generated by attrition processes which are typically far more coarse. However,
74 even within the particles generated from combustion and other high temperature sources, there may
75 well be different modal diameters associated with different sources or even multiple modes
76 associated with an individual source (Vu et al., 2015a). For example, exhaust emissions from diesel
77 engines typically comprise both a nucleation mode and an overlapping Aitken mode, reflecting in

78 the former case particles comprised mainly of condensed lubricating oil formed after the
79 combustion process, and in the latter case, solid carbonaceous particles formed within the
80 combustion process (Shi and Harrison, 1999; Alam et al., 2016).

81
82 After their emission, particle size distributions are also liable to change through dynamic processes.
83 These include evaporation which causes particles to shrink without changing the overall number,
84 condensation which causes particles to grow without a change in total number, coagulation which
85 also causes growth but reduces the total particle number, and deposition which causes a reduction in
86 number and is a strong function of the particle size.

87

88 There are detailed assessments of the concentrations and size distributions of nanoparticles in the
89 rural atmosphere (Van Dingenen et al., 2004; Asmi et al., 2011), and of their dynamics during
90 atmospheric transport (Beddows et al., 2014), urban studies have been limited. There has been
91 much research on emissions from road transport (Zhu et al., 2002a, b; Kumar et al., 2011), with
92 some attention given to shipping (Gonzalez et al., 2011) and to general modelling of sources
93 (Posser and Pandis, 2015). However, most urban measurement studies have been limited to a single
94 site (Morawska et al., 1998; Wang et al., 2011; Brines et al., 2015), although in a few instances
95 more sites have been considered (Karl et al., 2016) but not as part of a concerted campaign.

96
97 Within this study, particle number size distributions were measured simultaneously by electrical
98 mobility spectrometers at five separate sites across London and the size distributions are compared
99 with a view to gaining a better understanding of the sources and processes affecting particles in the
100 urban atmosphere.

101
102
103

104 2. **EXPERIMENTAL**

105
106 Data were collected from 27 January 2017 to 16 February 2017 as part of the second campaign of
107 the FASTER project. Data recovery was high (100%, or close) at all sites except Westminster
108 University, where good SMPS data were collected on only three days, January 30 and 31 and
109 February 1, 2017.

110

111 2.1 **Sampling Sites**

112 Data were collected at five sampling sites in total, three of which were established specifically for
113 the FASTER campaign, Westminster University, Regent's University and BT Tower. The other
114 two sites (London Marylebone Road and London North Kensington) collect data as part of the
115 national Automatic Urban and Rural Network. The site locations (seen in Figure 1) and
116 characteristics are as follows:

- 117 • *Marylebone Road.* Air sampling equipment is housed in a large kerbside cabin on the sidewalk
118 of a busy central London street canyon with an inlet approximately 2.5 m above ground-level
119 (agl). The adjacent six-lane highway carries around 80,000 vehicles per day. The highway is
120 relatively straight and runs almost due east-west (angle 80° from north). The buildings on
121 either side of the highway are around six storeys in height giving a street canyon aspect ratio of
122 approximately 1:1.
- 123 • *Westminster University.* Air sampling instruments were located on the roof of the Westminster
124 University building, almost directly above the Marylebone Road air sampling site on the
125 southern side of the street. The instruments were housed in a temporary enclosure located
126 approximately 26 m above street level and 4.5 m from the front edge of the roof where it
127 overlooks the road, and with an inlet 1.5 above the roof.
- 128 • *Regent's University.* A temporary enclosure for the instruments was located on the roof of
129 Regent's University which is an isolated building within Regent's Park due north (i.e. 360°) of
130 the Marylebone Road and Westminster University sites. The only highway lying between

Marylebone Road and the Regent's College site is a lightly trafficked road within Regent's Park. The distance between the Westminster University and Regent's University sites is estimated at 380 m. The instruments were located 16 m agl and 1 m from the edge of the roof.

- *London North Kensington.* Instruments were sited in a permanent cabin located within the grounds of a high school in a lightly trafficked suburban area of central London, with an inlet approximately 2.5 m agl. The air pollution climate at this site, often taken as representative of the background air quality within central London, has been characterised in detail by Bigi and Harrison (2010).

- *BT Tower.* Instruments were sited on level T35 at approximately 160 m agl on a narrow tower which rises well above the surrounding buildings on a quietly trafficked street approximately 380 m to the south of Marylebone Road. The site was used extensively in the REPARTEE experiment (Harrison et al., 2012a).

2.2 Sampling Instruments

The instruments (Table 1) were operated according to Wiedensohler et al. (2012) guidelines with the omission of a dryer at three sites (discussed later), and calibrated and intercompared both before and after the sampling campaign. Small correction factors ($< 5\%$) were applied to CPC (condensation particle counter) data as a result of the intercomparison. SMPS (scanning mobility particle sizers) data were analysed using the AIM9 and AIM10 software provided by TSI as appropriate to the instrument. The national network sites (Marylebone Road and North Kensington) are fitted with diffusion dryers according to EUSAAR/ACTRIS protocols (Wiedensohler et al., 2012), but the other sites were not. The particle size ranges measured were 14.9-615.3 nm at Westminster University, Regent's University and BT Tower, 16.55-604.3 nm at Marylebone Road and North Kensington, and a further system with a short DMA (differential mobility analyses) gave 4.96-145.9 nm at Regent's University.

157 It was not possible to use identical SMPS systems at each site. The variants used are shown in
158 Table 1. We expect little difference between the long column classifiers (TSI 3081) used at all sites
159 but with different platforms (TSI 3080 and TSI 3082) and CPCs (TSI 3775 and 3776). Differences
160 are expected to be minimal as platform-specific software was used to invert the data and both the
161 CPC are butanol-based, with only slightly different lower cut-points which were well outside of the
162 range of measured particles. At the Regent's University site, both a long DMA (3081) and short
163 column DMA (3085) were utilised and the data were merged to give a single continuous size
164 distribution from 6 nm to 650 nm. A possible cause of divergence is the fact that two of the sites
165 (Marylebone Road and North Kensington) used diffusion dryers according to the EUSAAR/
166 ACTRIS Protocol. The dryers were tested when installed and showed very low particle losses (less
167 than 5%) and no significant change to particle size distributions (NPL, 2010). The dryer may,
168 however, affect the particle size distribution due to the hygroscopicity of certain kinds of particles.
169 Vu et al. (2015b) reviewed hygroscopic growth factors for submicron aerosols from different
170 sources. Their data are difficult to extrapolate to this study as measurements of hygroscopic growth
171 are typically made at very high relative humidities, normally around 90%. Even at 99.5% relative
172 humidity, the growth of particles of less than 100 nm sampled from the atmosphere is relatively low
173 (Vu et al., 2015b). Consequently, a reduction in humidity from 88% typical of the campaign to the
174 values of 30-40% achieved in the dryer would be expected to have only a small effect on particle
175 sizes especially as fresh traffic-generated particles which comprise a large proportion of the sub-
176 micrometre particulate matter in the urban atmosphere are hydrophobic and therefore undergo zero
177 or very limited growth in humid atmospheres.

178

179 **2.3 Weather Conditions During the Campaign**

180 Wind speed and direction data were taken from Heathrow Airport to the west of London to reflect
181 the synoptic flow minimally affected by local building effects. At the start of the campaign (27
182 January 2017) the wind direction was easterly and moved to southerly by January 29th, briefly

183 passing through northerly before returning to a southerly circulation between January 31 and
184 February 3rd. During this time, wind speeds were typically around 4 m s^{-1} and temperatures mild
185 for the time of the year (mostly $6\text{-}10^\circ\text{C}$). From February 4th to 8th there was a period of lower
186 wind speeds ($1\text{-}4 \text{ m s}^{-1}$) with variable wind directions and low nocturnal minima temperatures
187 (down to 1°C). From February 8 – 12th, a period of northerly winds (speeds of $3\text{-}5 \text{ m s}^{-1}$) and lower
188 temperatures ($1\text{-}3^\circ\text{C}$) without appreciable diurnal variation occurred. After February 12th, the
189 winds came from the east moving to south-westerly by February 17th, with wind speeds variable
190 (between 0 and 6 m s^{-1}) and temperatures steadily rising to daily maxima of 12°C .

191

192 The mixed layer heights (MLH) were determined from Vaisala CL31 ceilometer data collected at
193 the Marylebone Road site (Figure 1, Table 1). The observed 15 s (10 m gates) aerosol attenuated
194 backscatter profiles were pre-processed (Kotthaus et al., 2016) prior to using the CABAM
195 algorithm (Kotthaus and Grimmond, 2018) to determine 15 min intervals MLH. The multiple
196 aerosol layers (e.g. nocturnal residual layers) in the atmosphere are detected (Kotthaus and
197 Grimmond, 2018; Kotthaus et al., 2018). Here the lowest detected layer is analysed. At times the
198 MLH cannot be detected (e.g. during rain or very weak gradients in attenuated backscatter), but a
199 residual layer might still be indicated. The ceilometer detects periods of precipitation, including
200 events that may not be recorded by ground-based stations (e.g. insufficient to trigger a tipping
201 bucket rain-gauge).

202

203 During the campaign the observed MLH varied from a daily minimum of 45 m agl to a daily
204 maximum of 1312 m agl with an overall 15 min average (median) of 421 (382) m agl . The daily
205 average (median) maximum MLH was 777 (695) and minimum was 194 (197) m agl . The daily
206 range and the amount of data available per day are shown in Figure S1.

207

208

209 **2.4 Modal Analysis of Size Distributions**

210 Modes were fitted to the 15 min data obtained at Marylebone Road, Regent's and Westminster
211 Universities using curve fitting and data analysis software "Fityk (version 1.3.1)" developed by
212 Wojdyr (2010). In the present analysis, a standard peak function (equation 1) was used to
213 disaggregate the size distributions into lognormal modes:

$$P_i = A_i \cdot \exp \left[- \left(\frac{\ln(D/c_i)}{W_i} \right)^2 \right] \quad (1)$$

214 By fitting linear a combination of n peaks ($P_1 + P_2 + \dots + P_i + \dots + P_n$) to the number size
215 distributions, the following information was calculated: 1) amplitude A_i and location of $dN/d\log D$ at
216 the mode of the distribution c_i , 2) area under the curve (nm cm^{-3}), and 3) width of the lognormal
217 curve W_i .

218

219 **3. RESULTS AND DISCUSSION**

220 **3.1 Particle Size Distributions**

221 A time series of total particle number concentrations from the SMPS instruments appears in Figure
222 2. A strong diurnal variation is seen at all sites and is exemplified by the average daily variation
223 shown in Figure 3.

224

225 The data stratified by the wind direction measured at London Heathrow airport (LHR) (Figure 4)
226 were used to perform the modal analysis. The log normal modes fit to the size distribution were
227 used to provide insights into the separate modes contributing to a measured size distribution.

228 Although most measurements could be fit with three separate modes some distributions were best
229 fit with only two modes. An example of a three mode fit of a size distribution from North
230 Kensington appears in the data for the 270° wind sector at this site (Figure 5). It may be seen that
231 using three modes gives a very good overall fit to the data. The details of the modes fitted and their
232 relative magnitude and breadth appear in Table S1.

233

234 The Marylebone Road sampling site is located in a heavily trafficked (approx. 80,000 vehicles per
235 day) street canyon. The canyon is aligned almost east-west and the sampling site is at kerbside on
236 the southern side of the street. The canyon has a height to width ratio of ~ 1 consequently we expect
237 skimming flow when flow is perpendicular, with one or more vortices established in the canyon
238 (Oke et al. 2017). When there is one vortex, the sampler is exposed to freshly emitted traffic
239 contaminants when the wind above the canyon is from the south (Figure 6). Particle number
240 concentration on Marylebone Road is highest for the 225° and 270° wind sectors (Figure 4a) when
241 traffic-generated pollutants are carried efficiently to the sampler. When winds have a northerly
242 component such as those for 0° and 45° in Figure 4a, the air reaching the sampler is typical of
243 background air from north London and peak concentrations fall by a substantial margin. The
244 particle size data from Marylebone Road (Table S1) show no strong effect of wind direction on the
245 modal diameter for the first fitted mode in the distribution. The average diameter for the 180° and
246 225° wind sectors are 21.4 nm while for the 0° and 45° sectors they are 22.9 nm. The second and
247 third mode in the distribution are far more sensitive to wind direction, with the southerly traffic-
248 dominated wind directions showing modes at around 32 and 76 nm as opposed to 56 nm and 263
249 nm for the northerly mode data. The former values compare well with modes in the number
250 distribution of around 20 nm and 50 nm previously attributed to the nucleation mode and Aitken
251 mode particles respectively from engine exhaust when sampled at Marylebone Road, with data
252 analysed by Positive Matrix Factorization (Harrison et al., 2011).

253

254 The Westminster University sampling site is 26 m higher and slightly displaced (~ 8 m) horizontally
255 from the Marylebone Road air sampling station. The observations at roof level are influenced by
256 the flow separation over the roof, if the air is entering or exiting the canyon, and the background
257 concentrations. The particle size data (Table S1) indicate a nucleation mode very similar in size to
258 that observed within the street canyon at the Marylebone Road site. Concentrations are elevated for
259 the 135° and 180° wind bearings suggesting that enhanced concentrations occurring within the

260 canyon on southerly winds are also elevated at the Westminster University sampler but the dataset
261 is very small and hence not included in Figure 4. The second mode appears to be broadly similar in
262 size to that at Marylebone Road and falls within the range of modal diameters measured at
263 Marylebone Road. Similarly, the third mode falls within the rather variable range also seen at
264 Marylebone Road.

265

266 The North Kensington site is widely taken as representative of the background air pollution climate
267 in central London (Bigi and Harrison, 2010; Bohnenstengel et al., 2015). At this site, the size of the
268 first mode in the size distributions is remarkably constant at 22-26 nm which is slightly larger than
269 that observed at Marylebone Road. The second mode is also less variable than at most other sites
270 and broadly within the range of the second mode sizes at Marylebone Road (see Table S1). The
271 third mode is highly variable in size with wind direction but again broadly comparable to the data
272 from Marylebone Road. The Beddows et al. (2015) Positive Matrix Factorization of particle
273 number size distributions data from this site identified four factors contributing to the particle
274 number size distributions: a secondary component accounting for 4.4% of particle number with a
275 mode at around 250 nm, an urban background factor (43% of particle number) peaking at around 50
276 nm, a traffic component (44.8% of particle number) peaking at around 30 nm and a regional
277 nucleation component (7.8% of particle number) peaking at 20 nm. The regional nucleation
278 component showed a strong seasonality with greatest prevalence in the summer months and is
279 thought unlikely to have contributed significantly during the period of this campaign. This was a
280 winter campaign without clear evidence of nucleation leading to new particle formation at any of
281 the sites. A subsequent paper has investigated the factors influencing nucleation at three related
282 sites, including North Kensington and Marylebone Road (Bousiotis et al., 2018). Consequently, the
283 first mode observed in our current study is very comparable to the traffic mode observed by
284 Beddows et al. (2015), and the second mode corresponds strongly to the urban background factor
285 identified by Beddows et al. (2015) who associated this factor with aged traffic emissions and wood

286 smoke, the latter of which is unlikely to have influenced the size distribution at Marylebone Road
287 significantly.

288

289 **3.2 Particle Shrinkage**

290 Previous London work has shown the tendency of nucleation mode traffic-generated particles
291 sampled within Regent's Park to have shrunk by evaporation at rates of on average 0.13 nm s^{-1}
292 (Harrison et al., 2016) while particles in the regional atmosphere typically undergo condensational
293 growth at a rate of about $0.6\text{-}0.9 \text{ nm h}^{-1}$ (Beddows et al., 2014). This reflects an initial local rapid
294 loss of more volatile hydrocarbons, followed by a subsequent slower condensation of low volatility
295 species formed by atmospheric oxidation in the regional atmosphere.

296

297 Under southerly flows the Regent's University site is downwind of Marylebone Road (Fig. 1). The
298 modal diameters measured at Regent's University in the nucleation mode (Table S1) are clearly
299 indicative of a shrinkage of particle diameter for the wind sectors 180° , 225° and 270° ,
300 corresponding to air having passed over Marylebone Road. These data show that the nucleation
301 mode is shrinking from a diameter in the range of 21-24 nm at Marylebone Road, and 22-24 nm at
302 Westminster University to a diameter of 14, 9 or 12 nm at the Regent's University site. In this case,
303 particle shrinkage seems to be limited to those three wind sectors, with possibly some shrinkage in
304 the 45° wind sector, but particles in other wind sectors retain broadly similar diameters to those
305 measured at Marylebone Road and Westminster University. The second particle mode and third
306 particle mode (where identifiable) at Regent's University are broadly similar and considerably
307 larger than those measured at Marylebone Road or in the limited dataset at Westminster University.

308

309 In our earlier studies of the evolution of particle sizes between Marylebone Road and Regent's Park
310 (Harrison et al., 2016), the nucleation mode in the Marylebone Road size distributions lay between
311 20-24 nm (i.e. very similar to this study). In Regent's Park this had reduced to within the range of

312 6-11 nm with the largest sizes measured in the 0° wind sector and the smallest in the 180° wind
313 sector. The current data show a similar general pattern, although the extent of size reduction is
314 smaller. The travel distance to the Regent's University site is shorter, hence accounting in part for
315 less shrinkage, but the overall shrinkage rate in the current study (0.04 nm s^{-1}) was smaller than
316 previously (0.13 nm s^{-1}) (Harrison et al, 2016). This is probably explained by two factors. Firstly,
317 with warmer mean air temperatures (12-18°C) evaporation would be enhanced, and secondly, as the
318 site used for collection of the data described in the Harrison et al. (2016) study was in the centre of
319 the park and further from any major highways than the Regent's University site, it may have
320 experienced lower vapour concentrations. Consequently, the two datasets appear highly consistent
321 with one another.

322

323 Previous BT Tower site observations have reported loss of $< 20 \text{ nm}$ particles (Dall'Osto et al.
324 2011). This loss was greatest when atmospheric turbulence levels were lowest and hence the time
325 for ground to sampling height (160 m) transport greatest. That analysis is not repeated in this study.
326 However, the nucleation mode size (Table S1) has grown slightly from the sizes measured at
327 Marylebone Road for the nucleation mode. It is notable that unlike the earlier results, the amplitude
328 of this mode at the BT Tower was substantial and slightly larger than that observed at the ground-
329 level background North Kensington site suggesting that there was generally good coupling between
330 ground-level and the Tower site. It is notable that the first mode diameter with greatest amplitude
331 was for the 270° sector (Figure 4d); this is discussed later. The particle size distribution associated
332 with the 225° wind sector had only one mode at 40 nm suggestive of the second solid particle mode
333 with complete evaporation of the semi-volatile nucleation mode.

334

335 Earlier studies have shown that particle number concentrations ($< 100 \text{ nm}$) in a street canyon
336 (Olivares et al., 2007) and urban air (Hussein et al., 2006) increase with reducing temperature. This
337 is consistent with the semi-volatility of nucleation mode particles from road traffic (Harrison et al.,

2016), and consequently it would be expected that the particle size distribution as well as the number concentration would be affected by ambient temperature. To investigate this, the size distributions collected in the lowest quartile of air temperatures (1.1 to 3.8°C) were compared with those in the highest quartile of temperature (9.1 to 11.8°C). This showed generally higher concentrations associated with the higher temperatures, and a clearer nucleation mode at higher temperatures, at all sites, and most notably at Marylebone Road. Such behaviour is contrary to expectations, as greater evaporative losses would be expected at higher temperatures, reducing the magnitude of the plot, or shifting the mode to smaller sizes. To understand this effect more clearly, wind directions with the coldest and hottest quartiles of temperature are analysed. The coldest periods all occurred during northerly flows (270 to 90°) and >85% of highest quartile of temperatures occur during southerlies (90 to 270°). The behaviour, especially at Marylebone Road and Regent's University therefore appears to be determined predominantly by synoptic wind conditions. For Marylebone Road, the street canyon flow (Figure 6) is the dominant influence and at Regent's University the traffic sources are most proximate with southerly flows.

352

3.3 Particle Number Concentration (CPC) Data

Average diurnal variations of total particle number count derived from the Condensation Particle Counters produced using the Openair Software Package (Carslaw and Ropkins, 2012) appear in Figure S2. At both Marylebone Road and Westminster University, these show a peak occurs between midnight and 6 am before reducing and then rising to a second peak in the afternoon. CPC concentrations at these sites far exceed those at Regent's University and the BT Tower, whereas integrated counts from the SMPS instruments were considerably smaller and showed a diurnal variation broadly similar to that expected for road traffic emissions (Figure 3). While it is quite normal for the CPC to give a higher count than the SMPS since it measures over a wider size range and may have lower internal losses (although the SMPS data analysis software corrects for internal losses), the ratio of CPC to SMPS is in our experience (e.g. Shi et al., 2001) typically around two,

364 but this value was significantly exceeded episodically, especially at Westminster University (Figure
365 S3). The overall pattern of CPC to SMPS ratios (Figure 7) shows that some of the highest ratios
366 were at Regent's University with two individual occasions exceeding 13. Some high peak values
367 were observed at Westminster University during the short SMPS time series. Wood burning is
368 recognised as an influential source of particles in London (Harrison et al, 2012b; Crilley et al.,
369 2015), and has a diurnal profile with higher concentrations typically at night. During the ClearfLo
370 winter campaign the BT Tower was influenced substantially by wood smoke irrespective of
371 boundary layer depth (Crilley et al, 2015). Since the BT Tower site was predominantly within the
372 mixed layer during the 2017 campaign (Figure S1) and the CPC/SMPS average ratios at the Tower
373 show little nocturnal elevation, we consider it unlikely that wood smoke explains our observations.
374 Furthermore, particle size distributions associated with biomass burning are typically larger than
375 those from road traffic, and outside of the sub-15 nm size range (Vu et al., 2015a). The occurrence
376 of the maximum in this behaviour at nighttime (3-4am) suggests that other heating-related
377 emissions (e.g. from natural gas combustion) are not the source.

378

379 To evaluate this phenomenon more closely, the Black Carbon data were examined. These are
380 typically taken as a good tracer of diesel exhaust which is expected to be the main source of the
381 particle number count. The diurnal variation in Black Carbon (Figure S4) conformed reasonably
382 well to that expected for a traffic-generated pollutant with Marylebone Road concentrations far
383 exceeding those at the other sites and showing a typical traffic-associated pattern. Particle number
384 (derived from the CPC) to Black Carbon ratio (Figure S5) shows huge diurnal variability similar to
385 that seen in the ratio of particle number count from the CPC to that derived from the SMPS. We
386 infer from this behaviour that a large number of particles smaller than the lower limit of the SMPS
387 and above the lower limit of the CPC (i.e. 2.5-14.9 nm for the 3776 instrument at Westminster
388 University and Regent's University; 4-14.9 nm for 3775 instrument at BT Tower; and 3-16.55 nm
389 for 3025 instrument at Marylebone Road) were present in the atmosphere. Both the mean ratio of

CPC to SMPS (Figure S3) and CPC to Black Carbon (Figure S6) have ratios that are greatest in the early morning (midnight to 6 am). This is unexpected for the CPC/SMPS ratio, as the contribution of traffic relative to regional aerosol is expected to be least and the coarser regional aerosol contains few particles in the size range below the lower limit of the SMPS instrument. Similarly, for the Black Carbon data, one would expect that if traffic is the main source of particles measured by the CPC, the latter would show a diurnal fluctuation like that of Black Carbon, which in London arises mostly from traffic emissions. Consequently, it seems likely that nucleation processes favoured by the cooler temperatures and lower condensation sink in the early hours of the morning are creating large numbers of particles in the range of 2.5-15 nm mobility diameter. These are forming as air moves away from the traffic source and hence are greatest at the rooftop Westminster University site and have diminished to some extent by coagulation or re-evaporation by the time they reach the Regent's University site which still shows a marked elevation in particle number to Black Carbon ratio in the earlier hours of the morning compared to the Marylebone Road site.

Such behaviour is somewhat unexpected and a review of papers in which vertical gradients in particle number count have been measured above roadside sites showed no earlier evidence of such behaviour (Lingard et al., 2006; Agus et al., 2007; Nikolova et al., 2011; Ketzel et al., 2003; Longley et al., 2003; Kumar et al., 2008a, b; Kumar et al., 2009; Li et al., 2007; Vakeva et al., 1999; Zhu et al., 2002b; Wehner et al., 2002). However, evidence is seen in some of Villa et al.'s (2017) observations, particle number count increased with height up to around 10 m above a multi-lane highway. The authors reported this unexpected pattern for some ascents/descents and attributed it to exhaust tubes of heavy duty trucks tending to project vertically upwards and to be located at a height of several metres above ground. They suggest this is not the case in urban canyons.

Another possibility arises from the report of Rönkkö et al. (2017) that large numbers of sub-4 nm particles are observed in the exhaust of some diesel engines and the observation by Nosko et al. (2017) of substantial numbers of similarly sized particles amongst emissions from brake wear. Kontkanen et al. (2017) reported observations of sub-3 nm particles from many sites, the highest concentrations being in urban locations. The diurnal and regional variations did not relate clearly to photochemistry and it was concluded that sub-3 nm particle concentrations are affected by anthropogenic sources of precursor vapours. The correlation of sub-3 nm particle concentrations in Helsinki with nitrogen oxides suggested a link with traffic emissions. Shi et al. (2001) measured particles of >9.5 nm by SMPS, >7 nm by CPC and >3 nm by ultrafine CPC, finding large numbers of particles in urban air in the ranges 3-7 nm and 3-9.5 nm by differences of counts. Ratios of CPC (>3 nm):SMPS (>9.5 nm) were highly variable, but typically around 4. Clear links to road traffic were seen, with drive-by experiments showing large numbers of particles in the 3-7 nm range in the exhausts of both diesel and gasoline vehicles (Shi et al., 2001). Nanoparticles were also produced in the plume downwind of a stationary combustion source (Shi et al., 2001). Herner et al. (2011) measured the size distribution of particles emitted from vehicles equipped with diesel particle filters, and with diesel filters and selective catalytic reduction. The dominant mode in the size distribution was at 10 nm diameter and comprised particles with a high fraction of sulphate. In highway and roadside measurements in Helsinki, Enroth et al. (2016) measured particle size distributions with a dominant mode at 10 nm diameter. Such particles would be largely below the lower threshold for counting by the SMPS but not the CPC. It is plausible that during the cooler hours of the night a tail of <2.5 nm particles might be subject to condensational growth if the co-emitted vapour were to be supersaturated in the atmosphere within the street canyon. The dominance of a 10 nm mode in the size distribution would appear to be the most plausible explanation for the high number concentration of particles observed at the Westminster University rooftop location and the apparent transport of a substantial proportion of such particles to the Regent's University measurement site. While this can explain the typically high CPC/SMPS ratios

441 observed, it does not explain their diurnal variation. This appears to require growth of sub-2.5 nm
442 particles into the range measured by CPC in the cooler, more humid nocturnal conditions. Rönkkö
443 et al. (2006) and Schneider et al. (2005) studied the formation of mechanisms and composition of
444 diesel exhaust nucleation particles in the laboratory and during car chasing. They conclude that
445 formation of nucleation mode particles depends upon formation of sulphate nuclei upon which
446 hydrocarbons condense, consistent with earlier studies of Shi and Harrison (1999) and Shi et al.
447 (2000) conducted in our laboratory. Factors favouring nucleation mode particle formation were
448 found to be low temperature and high humidities, consistent with field measurements made on
449 Marylebone Road (Charron and Harrison, 2003). Both factors prevail at nighttime, probably
450 contributing to the relative increase in 2.5–15 nm diameter particles seen most notably between
451 midnight and 6am (Figure S3). Salimi et al. (2017) reported nocturnal new particle formation
452 events in Brisbane, Australia, finding that air masses associated with nocturnal events were
453 typically transported over the ocean before reaching their sampling site, but the relevance to our
454 study is unclear, although the maritime air might sometimes be expected to show lower temperature
455 and higher humidity than that from the land.

456

457 Support for our observations also comes from the very detailed measurement and modelling study
458 of Choi and Paulson (2016). Measuring particle number size distribution downwind of a major
459 highway, they found a positive anomaly in particle number within the first 60 m of the plume peak,
460 as the peak for the small particles appeared further downwind than the peak in accumulation mode
461 particles. They attributed this to growth of unmeasured sub-5.6 nm particles into the smallest
462 measurable size range and suggested condensational growth or self-coagulation as the mechanism
463 (Choi and Paulson, 2016). Kerminen et al. (2007) measuring near a major road in Helsinki reported
464 particle growth by condensation to be a dominant process during the road-to-ambient evolution
465 stage at nighttime in winter. They inferred that under such conditions (low wind speeds with a
466 temperature inversion), traffic-generated particle numbers were enhanced and could affect

467 submicron particle number concentrations over large areas around major roads. The distance scales
468 for such processes in both studies (Choi and Paulson, 2016; Kerminen et al., 2007) were within 100
469 m of source under the conditions of measurement but might conceivably extend over greater
470 distance scales. Similar processes of particle evolution within an aircraft exhaust plume have been
471 reported by Timko et al. (2013).

472

473 Pushpawela et al. (2018) report a phenomenon of hygroscopic particle growth at nighttime, which
474 can potentially be mistaken for new particle formation. This phenomenon was observed between
475 0.5-5.0 hours after sunset, peaking at 3.5 hours (Pushpawela et al., 2018). This would not appear to
476 explain our observations, where the peak in N/SMPS and N/BC plots (Figures S2 and S5) is
477 greatest at 3-4 am local time, which in London in winter is some 10-11 hours after sunset.
478 Additionally, such a phenomenon would be expected to be unrelated to local traffic emissions, and
479 hence more uniform across the various sites.

480

481 **3.5 Spatial Distribution of Particles – Horizontal and Vertical**

482 Figure 2 shows the time series of particle concentrations from the SMPS instruments throughout the
483 campaign. Clearly, as expected, the Marylebone Road site shows the highest concentrations through
484 the campaign period due to its proximity to the road traffic source. The other sites tend to track one
485 another quite closely with no consistent ranking of concentrations. There are periods such as
486 February 1st to 3rd when Regent's University well exceeds North Kensington, but at other times,
487 they are very similar (e.g. 10 – 12 February), or periods when North Kensington exceeds Regent's
488 University (e.g. 7 February) but these are few. In the former period (1 – 3 February), winds were
489 southerly and concentrations at Regent's University would be enhanced by passage of air across
490 Central London, including Marylebone Road. In the situation where concentrations were similar (10
491 – 12 February), winds were in the northerly sector, giving relatively low concentrations at all sites,
492 and rather little spatial variation. The temporal pattern at all sites showed substantial similarity

493 overall (Figure 2), including diurnal patterns (Figure 3), although the magnitude of concentrations
494 varied.

495

496 A time series of CPC particle number concentrations (Figure 8) showed that under most conditions ,
497 the number count was lowest at the BT Tower site, and that the number count at Westminster
498 University frequently exceeded that at Marylebone Road, with Regent's University lower, but
499 above the concentration at the BT Tower (Figure 8). During the period of northerly winds (8 – 12
500 February), all sites showed low concentrations with Regent's University and BT Tower similar for
501 much of the time, as for the SMPS data (Figure 2). The highest CPC count concentrations during
502 the latter were measured at Westminster University (Figure 9) which was downwind of Marylebone
503 Road at those times. The similarity seen between Westminster University and Marylebone Road
504 for much of the campaign, with concentrations far in excess of those at BT Tower is strongly
505 suggestive of continuing particle growth into the size range 2.5–14.9 nm at Westminster University
506 with re-evaporation occurring before reaching the elevated BT Tower site, as previously observed
507 by Dall'Osto et al. (2011). Elevations in N/BC data were seen at the BT Tower site (Figure S4 and
508 S6) but these occurred mainly during the morning rush hour period, presumably due to fresh traffic
509 emissions, rather than overnight as at the other sites (Figure S6).

510

511 Figure 2 suggests that vertical gradients between the proximate Regent's University and BT Tower
512 sites were small in SMPS count (Figure 2), but at certain times were substantial in the CPC count
513 (Figure 9). The particle size distributions measured at the BT Tower (Figure 4d) differ from
514 Marylebone Road and North Kensington (Figure 4a and b) in having no obvious mode in the
515 nucleation size range at 20 – 30 nm, a feature shared with Regent's University (Figure 4c). Only
516 during westerly winds (270°) does the BT Tower show such a mode (Figure 4d), while at Regent's
517 University (Figure 5) the 270° wind direction also shows differences from the others with a mode at
518 below 20 nm. Anomalous behaviour in this wind sector is also observed at North Kensington

(Figure 4b), and at Marylebone Road. The most pronounced nucleation mode peak is associated with the 270° and 225° wind directions. In the Marylebone Road case, these wind directions are almost parallel to the highway, which might explain the high concentrations and pronounced nucleation mode, but this explanation does not work for the other sites. A more likely explanation is that all sites are affected by emissions from Heathrow Airport which is to the west of London and has been recognised as a major source of nucleation mode particles associated with aircraft and road traffic emissions (Masiol et al., 2017). At a site 1 km from the northern boundary of Heathrow Airport, PMF factors attributed to aircraft (mode at <20 nm) and fresh road traffic emissions (mode at 18–35 nm) accounted respectively for 31.6% and 27.9% of particle number count in the warm season and 33.1% and 35.2% in the cold season (December 2014 – January 2015) data (Masiol et al., 2017). Heathrow Airport is located approximately 22 km from our Central London sites on a bearing of 255°. Keuken et al. (2015) measured a large elevation in concentrations of particles of 10–20 nm diameter attributed to aircraft emissions (emission studies are reviewed by Masiol and Harrison, 2014) at a site 7 km east of Schiphol Airport (Netherlands) and have shown by modelling and measurement that concentrations are elevated to considerably greater downwind distances. Similarly, Hudda et al. (2014) reported PNC to have increased 4 to 5 fold at 8 – 10 km downwind of Los Angeles International Airport (USA).

The size distributions have also been analysed according with mixed layer height (MLH), determined by ceilometer (Kotthaus and Grimmond, 2018). Both Marylebone Road (Figure S7) and Regent's University (Figure S8) have the highest concentrations associated with the deepest MLH class (>1000 m). This seems likely to be due to an association with southerly winds and the street canyon circulation. Whereas, North Kensington (Figure S9) has the highest concentrations during shallow MLH (< 100 m and 100 – 200 m) when dispersion is limited for the low altitude emissions. The most interesting behaviour is seen at the elevated (160 m) BT Tower site, which is consistent with Harrison et al. (2012a) and Dall'Osto et al. (2011). During the shallowest MLH (< 100 m) the

measurement site is above the inversion and the size distribution lacks an obvious nucleation mode (Figure S10). As the MLH deepens, a nucleation mode appears which dominates the size distribution for the deepest MLH categories (900 – 1000 m and >1000 m) with a mode at 20 – 30 nm, similar to that seen at Marylebone Road for the same MLH depths (Figure S7). The gradual transitioning of size distribution as the MLH deepens is consistent with the surface source (mainly road traffic) of nucleation mode particles, and their evaporative loss which increases with the timescale of vertical mixing to the height of the sampler, as reported by Dall'Osto et al. (2011), and the ultimate isolation of the sampler from ground-level emissions at the shallowest boundary layer heights, as observed by Harrison et al. (2012a).

554

3.6 Detailed Comparison of Marylebone Road, Westminster University and Regent's University

Unfortunately, a full dataset for the Westminster University site was only collected over the period January 30th to February 1st due to a late set-up of the instrument and a malfunction after February 1st. This period however merits closer examination as it is the only period where SMPS data were available for all three sites. For much of the time the SMPS data for the Westminster University site looks surprisingly similar to that of the Marylebone Road site despite the former being on the rooftop and the latter being within the street canyon. A detailed analysis hour by hour showed that out of 51 hourly observations, in 23 the amplitude of the mode ($dN/d\log D$) at Westminster University was within $\pm 20\%$ of that at Marylebone Road while in 25 cases the amplitude was greater at Westminster University than at Marylebone Road, and in just two cases the amplitude was smaller at Westminster University. In an attempt to explain this observation, the meteorological data for the periods of similar magnitude and of different magnitudes were compared but no systematic difference was seen in wind direction, air temperature or relative humidity between any of the periods. Wind directions were generally in a south-easterly to easterly

sector, mean temperatures around 8°C and relative humidity high (85 and 99%). The maximum MLH were low and there was a lot of rain (Figure S1).

In order to gain further insight, the time series of observations were plotted for this period and appear in Figure 9. The SMPS integrated number counts shown in Figure 9(a) show a remarkable similarity between Marylebone Road, Westminster University and Regent's University. For the first two days, Regent's University concentrations are lower than those from the other two sites, although on the third day they are very similar to those at Westminster University. On the first and last days, the peak concentrations at Marylebone Road exceed those at Westminster University but on the middle day (January 31st) the differences between these two sites are very small. The CPC particle number counts shown in Figure 9(b) are very similar to those at Marylebone Road on the first and last day but exceed those at Marylebone Road on January 31st. Concentrations at Regent's University are typically only around half or less of those measured at Westminster University. The magnitude of the CPC concentrations peaking at over 40,000 cm⁻³ is close to double the integrated SMPS counts which peak at a little over 20,000 cm⁻³ indicating a large number of particles in the size range below 14.9 nm.

However, the Black Carbon data (Figure 9c) have daytime concentrations at Marylebone Road that far exceed those at Westminster University and Regent's University, the latter sites tracking each other and having very similar concentrations. Since Black Carbon can be viewed as a conserved tracer of vehicle emissions over these small time and distance scales, the inference is that particle production must be continuing as the vehicle exhaust mixes upwards from the street canyon Marylebone Road site to the Westminster University rooftop site. The southerly wind directions likely associated with upward flow on the Westminster University canyon wall (Fig. 6) would carry vehicle exhaust past the Marylebone Road measurement station (south side of the road).

596 Air leaving the canyon and being entrained by the complex building roof flows could expose the
597 Westminster University sampler to air exiting the street canyon and to the general flow towards
598 Regent's University site (Fig. 6 and 1). Such behaviour is consistent with the observations of
599 particle growth in the sub-SMPS size ranges reported in the previous section extending into the
600 SMPS size range. This is similar to behaviour observed by Kerminen et al. (2007) in Helsinki who
601 observed not only possibly evaporation of some particles in the 7–30 nm range, but also on apparent
602 growth of nucleation mode particles into the 30–63 nm size range between sampling points at 9 m
603 and 65 m downwind of a highway. The results in Figure 9 are suggestive of a substantial growth of
604 nuclei into the range of the CPC at Westminster University.

605

606 **4. CONCLUSIONS**

607 The measurement of particle number size distributions in the atmosphere is resource intensive and
608 there have been rather few studies in which more than two samplers have been operated within a
609 city. Typically if there are two sites, one is a traffic-influenced site and the other urban background.
610 In this study, data have been collected at a total of five sites, although unfortunately the dataset
611 from the Westminster University site is limited to only a few days. Nonetheless, the dataset allows
612 some deep insights into the spatial distribution of particle sizes and number counts not only
613 horizontally but in the vertical dimension. Not unexpectedly, concentrations of particles at the
614 street canyon Marylebone Road site considerably exceed concentrations at other sites, but there are
615 nonetheless considerable similarities in diurnal profiles and the magnitude of concentrations at the
616 other, background sites.

617

618 One of the main motivating factors for this study was to confirm earlier observations of shrinkage
619 of the nucleation mode particles between traffic emissions on Marylebone Road and the downwind
620 site at Regent's University within Regent's Park. Particle shrinkage was observed within the
621 current study although at a slower mean rate (0.04nm s^{-1}) than in the earlier study (Harrison et al.,

2016) in which the mean shrinkage rate was 0.13nm s^{-1} . However, temperatures in the current study all fell below those in the earlier work of Harrison et al. (2016). Other factors may also have been influential. There have been marked changes in the road vehicle fleet in London between the two measurement campaigns. The earlier dataset as reported by Dall'Osto et al. (2011) and Harrison et al. (2016) was collected in 2006 at which time the sulphur content of diesel fuel was regulated at below 50 ppm. Between the two campaigns, the sulphur content of both gasoline and diesel motor fuels was reduced to below 10 ppm sulphur in order to facilitate the introduction of diesel particle filters from 2011 onwards. The incorporation of a diesel particle filter on EURO 5 and EURO 6 vehicles leads to a substantial overall reduction in particulate matter emissions but also a change in the hydrocarbon content of the particles. Secondly, the Regent's Park sampling site used for the 2006 measurements was at about double the distance from Marylebone Road compared to the Regent's University used in the latest study. This would allow for greater dilution of the traffic plume from Marylebone Road and other adjacent highways, leading to a greater reduction in vapour phase hydrocarbons at the more distant site causing an accelerated evaporation process. The reduction in fuel sulphur content in 2007 was accompanied by a marked change in the size distribution of particles emitted from road traffic, including a reduction in the nucleation mode particles (Jones et al., 2012). The work of Dall'Osto et al. (2011) also analysed data from the BT Tower, showing increasing evaporative loss of nucleation mode particles as the travel time from ground level to the sampling site on the Tower became longer with reduced atmospheric turbulence levels. Although that phenomenon has not been studied in detail in the latest dataset, the results are clearly consistent with such a process, and with an apparent total loss of the nucleation mode in particles associated with regional pollution sampled when the boundary layer top was below the sampling height on the tower.

Although the phenomenon of particle shrinkage had been seen in earlier work, there were two further major observations made in the current study which were not anticipated. The first, was the

648 clear influence of a major source to the west of London, almost certainly Heathrow Airport, upon
649 concentrations of nucleation mode particles. The association of an enhanced nucleation mode in the
650 270° or 225° sector is indicative of a major source of very fine particles, and the work of Masiol et
651 al. (2017) at a sampling site close to Heathrow Airport provides strong evidence for major
652 emissions both from aircraft engines and the large volumes of road traffic attracted by the airport.
653 Earlier research by Keuken et al. (2015) and Hudda et al. (2014) gives a clear precedent for
654 measurement of strongly elevated concentrations of very fine particles several kilometres
655 downwind of a major airport, but to our knowledge this is the first observations of concentrations
656 above urban background at a distance of 22 km from the centre of the airport.

657

658 The other observation which was wholly unexpected was of the very poor relationship between total
659 particle numbers measured by the Scanning Mobility Particle Sizers and the total particle numbers
660 measured by co-located condensation particle counters. While both the SMPS counts and co-
661 located Black Carbon measurements show a typical road traffic diurnal profile, the CPC data show
662 a quite different diurnal profile peaking at night. This is most evident in the ratios of CPC/SMPS
663 and CPC/BC seen at all sampling sites, with the exception of CPC/BC at the elevated BT Tower
664 site which does not show a nocturnal maximum, but peaks during the morning rush hour period.
665 Earlier studies such as that of Choi and Paulson (2016) and Kerminen et al. (2007) have reported
666 data consistent with such a phenomenon, but with very modest elevations in particle count
667 compared to those in the current data. The implication is of the presence of large numbers of
668 particles within the range of 2.5 – 15nm and hence observable with the CPC but below the lower
669 cut of the SMPS. It seems likely that such particles grow at night from very small nuclei and it
670 seems possible that the exceptional magnitude of this process within London results from the high
671 density of diesel traffic leading to substantial nocturnal concentrations of condensable vapours close
672 to the traffic source. A common feature to such observations appears to be its association with still
673 conditions on winter nights which lead to poor dispersion of vehicle emissions and a pool of vapour

674 co-emitted with traffic particles which becomes supersaturated as it cools in the ambient
675 atmosphere, leading to condensation on small nuclei when the general particle concentrations and
676 hence the condensation sink are relatively low in magnitude.

677

678 These very abundant particles within the 2.5 – 15 nm range are likely to prove ephemeral as they
679 would be expected to re-evaporate as the air mass dilutes away from source. However, the health
680 effects of exposure to particles within this range are poorly known and no recommendation can be
681 given as to whether health-related studies would be best to measure the particle size range covered
682 by the SMPS as is most typically performed at present, or whether CPC data going down to smaller
683 particles sizes would be more appropriate.

684

685 There are some additional general conclusions from the work. Firstly the results demonstrate the
686 dynamic behaviour of traffic-generated (and other) particles within the urban atmosphere. Our
687 earlier paper (Dall'Osto et al., 2011) referred to “remarkable dynamics”, and further remarkable
688 dynamic processes have been observed in the current study. Secondly, as this work has revealed
689 sources and processes that were not originally anticipated, although with the benefit of hindsight it
690 might have been possible to predict them, there is clearly a need for further detailed observational
691 studies of the behaviour of sub-100 nm particles within the urban atmosphere.

692

693 **ACKNOWLEDGEMENTS**

694 The authors are grateful to the management and staff of Westminster University, Regent's
695 University and British Telecom for access to their buildings for air sampling. They also express
696 gratitude to the National Centre for Atmospheric Science (NCAS) for the loan of sampling
697 instruments, and to Dr Paul Williams (NCAS) for facilitating the instrument intercomparison. The
698 operation of the ceilometers were supported by NERC ClearfLo, NERC AirPro, Newton Fund/Met
699 Office CSSP (SG, SK) and University of Reading. We acknowledge the support of KCL LAQN for

700 the instrument sites and support and the Reading Urban Micromet group for maintaining the
701 instruments, notably in this period Elliott Warren and Kjell zum Berge. The work was funded by the
702 European Research Council (ERC-2012-AdG, Proposal No. 320821) and the UK Natural
703 Environment Research Council (R8/H12/83/011) and a NCAS studentship (to JB).

704

705 **AUTHOR CONTRIBUTIONS**

706 DB, MA, JB and RX carried out the field measurements of particle size distributions, SK and SG
707 collected and interpreted the ceilometer data, and DB and AS carried out data analyses. RH led the
708 project and drafted the paper, with all co-authors contributing to subsequent enhancements.

709

REFERENCES

- Agus, E. L., Young, D. T., Lingard, J. J. N., Smalley, R. J., Tate, J. E., Goodman, P. S., and Tomlin, A. S.: Factors influencing particle number concentrations, size distributions and modal parameters at a roof-level and roadside site in Leicester, UK, *Sci. Tot. Environ.*, 386, 65-82, 2007.
- Alam, M. S., Rezaei, S. Z., Stark, C. P., Liang, Z., Xu, H. M., and Harrison R. M.: The characterisation of diesel exhaust particles – composition, size distribution and partitioning, *Faraday Discuss.*, 189, 69-84, 2016.
- Asmi, A., Wiedensohler, A., Laj, P., Fjaeraa, A.-M., Sellegri, K., Birmili, W., Weingartner, E., Baltensperger, U., Zdimal, V., Zikova, N., Putaud, J.-P., Marinoni, A., Tunved, P., Hansson, H.-C., Fiebig, M., Kivekas, N., Lihavainen, H., Asmi, E., Ulevicius, V., Aalto, P.P., Swietlicki, E., Kristensson, A., Mihalopoulos, N., Kalivitis, N., Kalapov, I., Kiss, G., Deleeuw, G., Henzing, B., Harrison, R. M., Beddows, D., O'Dowd, C., Flentje, H., Weinhold, K., Meinhardt, F., Ries, L., and Kulmala M.: Number size distributions and seasonality of submicron particles in Europe 2008-2009, *Atmos. Chem. Phys.*, 11, 5505-5538, 2011.
- Beddows, D. C. S., Dall'Osto, M., Harrison, R. M., Kulmala, M., Asmi, A., Wiedensohler, A., Laj, P., Fjaeraa, A.M., Sellegri, K., Birmili, W., Bukowiecki, N., Weingartner, E., Baltensperger, U., Zdimal, V., Zikova, N., Putaud, J.-P., Marinoni, A., Tunved, P., Hansson, H.-C., Fiebig, M., Kivekas, N., Swietlicki, E., Lihavainen, H., Asmi, E., Ulevicius, V., Aalto, P. P., Mihalopoulos, N., Kalivitis, N., Kalapov, I., Kiss, G., De Leeuw, G., Henzing, B., O'Dowd, C., Jennings, S. G., Flentje, H., Meinhardt, F., Ries, L., Denier Van Der Gon, H. A. C., and Visschedijk, A.J.H.: Variations in tropospheric submicron particle size distributions across the European Continent 2008-2009, *Atmos. Chem. Phys.*, 14, 4327-4348, 2014.
- Beddows, D. C. S., and Harrison, R. M., Green, D., Fuller, G.: Receptor modelling of both particle composition and size distribution data from a background site in London UK, *Atmos. Chem. Phys.*, 15, 10107-10125, 2015.
- Bigi, A., and Harrison R. M.: Analysis of the air pollution climate at a central urban background site, *Atmos. Environ.*, 44, 2004-2012, 2010.
- Bohnenstengel, S. I., Belcher, S. E., Aiken, A., Allan, J. D., Allen, G., Bacak, A., Bannan, T. J., Barlow, J. F., Beddows, D. C. S., Bloss, W. J., Booth, A. M., Chemel, C., Coceal, O., Di Marco, C. F., Dubey, M. K., Faloona, K. H., Fleming, Z. L., Furger, M., Geitl, J. K., Graves, R. R., Green, D. C., Grimmond, C. S. B., Halios, C. H., Hamilton, J. F., Harrison, R. M., Heal, M. R., Heard, D. E., Helfter, C., Herndon, S. C., Holmes, R. E., Hopkins, J. R., Jones, A. M., Kelly, F. J., Kotthaus, S., Langford, B., Lee, J. D., Leigh, R. J., Lewis, A. C., Lidster, R. T., Lopez-Hilfiker, F. D., McQuaid, J. B., Mohr, C., Monks, P. S., Nemitz, E., Ng, N. L., Percival, C. J., Prévôt, A. S. H., Ricketts, H. M. A., Sokhi, R., Stone, D., Thornton, J. A., Tremper, A. H., Valach, A. C., Visser, S., Whalley, L. K., Williams, L. R., Xu, L., Young, D. E., and Zotter, P.: Meteorology, air quality, and health in London: The ClearfLo project. *Amer. Meteor. Soc.*, 779-804, 2015.
- Bousiotis, D., Dall'Osto, M., Beddows, D. C. S., Pope, F. D. and Harrison, R. M.: Analysis of new particle formation (NPF) events at nearby rural, urban background and urban roadside sites, *Atmos. Chem. Phys. Discuss.*, <https://doi.org/10.5194/acp-2018-1057>, 2018.
- Brines, M., Dall'Osto, M., Beddows, D. C. S., Harrison, R. M., Gómez-Moreno, F., Núñez, L., Artíñano, B., Costabile, F., Gobbi, G. P., Salimi, F., Morawska, L., Sioutas, C., and Querol, X.:

761 Traffic and nucleation events as main sources of ultrafine particles in high insolation developed
762 world cities, *Atmos. Chem. Phys.*, 15, 5929-5945, 2015.

763

764 Carslaw, D. C., and Ropkins, K.: openair – An R package for air quality data analysis, *Environ.*
765 *Model. Softw.* 27-28, 52-61, doi:<https://doi.org/10.1016/j.envsoft.2011.09.008>, 2012.

766

767 Charron, A., and Harrison, R. M.: Primary particle formation from vehicle emissions during
768 exhaust dilution in the roadside atmosphere, *Atmos. Environ.*, 37, 4109-4119, 2003.

769

770 Choi W., and Paulson, S. E.: Closing ultrafine particle number concentration budget at road-to-
771 ambient scale: Implications for particle dynamics, *Aerosol Sci. Technol.*, 50, 5, 448-461, 2016.

772

773 Crilley, L. R., Bloss, W. J., Yin, J., Beddows, D. C. S., Harrison, R. M., Allan, J. D., Young, D. E.,
774 Flynn, M., Williams, P., Zotter, P., Prevot, A. S. H., Heal, M. R., Barlow, J. F., Hallios, C. H., Lee,
775 J. D., Szidat, S., and Mohr, C.: Sources and contributions of wood smoke during winter in London:
776 assessing local and regional influences, *Atmos. Chem. Phys.*, 15, 3149-3171, 2015.

777

778 Dall'Osto, M., Thorpe, A., Beddows, D.C.S., Harrison, R.M., Barlow, J.F., Dunbar, T., Williams,
779 P.I., and Coe, H.: Remarkable dynamics of nanoparticles in the urban atmosphere, *Atmos. Chem.*
780 *Phys.*, 11, 6623-6637, 2011.

781

782 Enroth, J., Saarikoski, S., Niemi, J., Kouse, A., Jezek, I., Mocnik, G., Carbone, S., Kuulivainen, H.,
783 Rönkkö, T., Hillamo, R., and Pirjola, L.: Chemical and physical characterization of traffic particles
784 in four different highway environments in the Helsinki metropolitan area, *Atmos. Chem. Phys.*, 16,
785 5497-5512, 2016.

786

787 Gonzalez, Y., Rodriguez, S., Guerra Garcia, J. C., Trujillo, J. L., and Garcia, R.: Ultrafine particles
788 pollution in urban coastal air due to ship emissions, *Atmos. Environ.*, 45, 4907-4914, 2011.

789

790 Harrison, R.M., Shi, J.P., Xi, S., Khan, A., Mark, D., Kinnersley, R., and Yin, J.: Measurement of
791 number, mass and size distribution of particles in the atmosphere, *Phil. Trans. R. Soc. Lond., A*,
792 358, 2567-2580, 2000.

793

794 Harrison, R.M., Beddows, D.C., and Dall'Osto, M.: PMF analysis of wide-range particle size
795 spectra collected on a major highway, *Environ. Sci. Technol.*, 45, 5522-5528, 2011.

796

797 Harrison, R.M., Dall'Osto, M., Beddows, D.C.S., Thorpe, A.J., Bloss, W.J., Allan, J.D., Coe, H.,
798 Dorsey, J.R., Gallagher, M., Martin, C., Whitehead, J., Williams, P.I., Jones, R.L., Langridge, J.M.,
799 Benton, A.K., Ball, S.M., Langford, B., Hewitt, C.N., Davison, B., Martin, D., Petersson, K.,
800 Henshaw, S.J., White, I.R., Shallcross, D.E., Barlow, J.F., Dunbar, T., Davies, F., Nemitz, E.,
801 Phillips, G.J., Helfter, C., Di Marco, C.F., and Smith, S.: Atmospheric chemistry and physics in the
802 atmosphere of a developed megacity (London): An overview of the REPARTEE experiment and its
803 conclusions, *Atmos. Phys. Chem.*, 12, 3065-3114, 2012a.

804

805 Harrison, R.M., Beddows, D.C.S., Hu, L., and Yin, J.: Comparison of methods for evaluation of
806 wood smoke and estimation of UK ambient concentrations, *Atmos. Chem. Phys.*, 12, 8271-8283,
807 2012b.

808

809 Harrison, R.M., Jones, A.M., Beddows, D.C., and Dall'Osto, M.: Evaporation of traffic-generated
810 nanoparticles during advection from source, *Atmos. Environ.*, 125, 1-7, 2016.

811

812 HEI: Understanding the Health Effects of Ambient Ultrafine Particles, Health Effects Institute, HEI
813 Perspectives 3, 2013.
814

815 Herner, D.H., Hu, S., Robertson, W.H., Huai, T., Chang, M.C.O., Riger, P., and Ayala, A.: Effect
816 of Advanced Aftertreatment for PM and NO_x Reduction on Heavy-Duty Diesel Engine Ultrafine
817 Particle Emissions, *Environ. Sci. Technol.*, 45, 2413-2419, 2011.
818

819 Hudda, N., Gould, T., Hartin, K., Larson, T.V., and Fruin, S.A.: Emissions from an international
820 airport increase particle number concentrations 4-fold at 10km downwind, *Environ. Sci. Technol.*,
821 48, 6628-6635, 2014.
822

823 Hussein, T., Karppinen, A., Kukkonen, J., Harkonen, J., Aalto, P.P., Hameri, K., Kerminen, V.-M.,
824 and Kulmala, M.: Meteorological dependence of size-fractionated number concentrations of urban
825 aerosol particles, *Atmos. Environ.*, 40, 1427-1440, 2006.
826

827 Jones, A.M., Harrison, R.M., Barratt, B., and Fuller, G.: A large reduction in airborne particle
828 number concentrations at the time of the introduction of “sulphur free” diesel and the London Low
829 Emission Zone, *Atmos. Environ.*, 50, 129-138, 2012.
830

831 Karl, M., Kukkonen, J., Keuken, M. P., Lutzenkirchen, S., Pirjola, L., and Hussein, T.: Modeling
832 and measurements of urban aerosol processes on the neighborhood scale in Rotterdam, Oslo and
833 Helsinki, *Atmos. Chem. Phys.*, 16, 4817-4835, 2016.
834

835 Kerminen, V.M., Pakkanen, T.A., Makela, T., Hillamo, R.E., Sillanpaa, M., Rönkkö, T., Virtanen,
836 A., Keskinen, J., Pirjola, L., Hussein, T., and Hameri, K.: Development of particle number size
837 distribution near a major road in Helsinki during an episodic inversion situation, *Atmos. Environ.*,
838 41, 1759-1767, 2007.
839

840 Ketzel, M., Wahlin, P., Berkowicz, R., and Palmgren, F.: Particle and trace gas emission factors
841 under urban driving conditions in Copenhagen based on street and roof-level observations, *Atmos.*
842 *Environ.*, 37, 2735-2749, 2003.
843

844 Keuken, M.P., Moerman, M., Zandveld, P., Henzing, J.S., and Hoek, G.: Total and size-resolved
845 particle number and Black Carbon concentrations in urban areas near Schiphol airport (the
846 Netherlands), *Atmos. Environ.*, 104, 132-142, 2015.
847

848 Kontkanen, J., Lehtipalo, K., Ahonen, L., Kangaslua, J., Manninen, H.E., Hakala, J., Rose, C.,
849 Sellegri, K., Xiao, S., Wang, L., Qi, X., Nie, W., Ding, A., Yu, H., Lee, S., Kerminen, V.-M.,
850 Petaja, T., and Kulmal, M.: Measurements of sub-3 nm particles using a particle size magnifier in
851 different environments: from clean mountain top to polluted megacities, *Atmos. Chem. Phys.*, 17,
852 2163-2187, 2017.
853

854 Kotthaus S, and Grimmond, C.S.B.: Atmospheric boundary layer characteristics from ceilometer
855 measurements Part 1: A new method to track mixed layer height and classify clouds, *Q. J. R.*
856 *Meteorol. Soc.*, <https://doi.org/10.1002/qj.3299>, 2018.
857

858 Kotthaus, S., and Grimmond, C. S. B.: Atmospheric boundary layer characteristics from ceilometer
859 measurements, Part 2: Application to London’s urban boundary layer, *Q. J. R. Meteorol. Soc.*,
860 <https://doi.org/10.1002/qj.3298>, 2018.
861

862 Kotthaus, S., Halios, C. H., Barlow, J. F., and Grimmond, C.S.B.: Volume for pollution dispersion:
863 London's atmospheric boundary layer during ClearfLo observed with two ground-based lidar types
864 Atmos. Environ., 190, 401-414, 2018.

865

866 Kumar, P., Fennell, P., and Britter, R.: Measurements of particles in the 5-1000 nm range close to
867 road level in an urban street canyon, Sci. Tot. Environ., 390, 437-447, 2008a.

868

869 Kumar, P., Fennell, P., Langley, D., and Britter, R.: Pseudo-simultaneous measurements for the
870 vertical variation of coarse, fine and ultrafine particles in an urban street canyon, Atmos. Environ.,
871 42, 4304-4319, 2008b.

872

873 Kumar, P., Garmory, A., Ketzel, M., Berkowicz, R., and Britter, R.: Comparative study of
874 measured and modelled number concentrations of nanoparticles in an urban street canyon, Atmos.
875 Environ., 43, 949-958, 2009.

876

877 Kumar, P., Robins, A., Vardoulakis, S., and Britter, R.: A review of the characteristics of
878 nanoparticles in the urban atmosphere and the prospects for developing regulatory controls, Atmos.
879 Environ., 44, 5035-5052, 2010.

880

881 Kumar, P., Ketzel, M., Vardoulakis, S., Pirjola, L., and Britter, R.: Dynamics and dispersion
882 modelling of nanoparticles from road traffic in the urban atmospheric environment – a review, J.
883 Aerosol Sci., 42, 580-602, 2011.

884

885 Kumar, P., Morawska, L., Birmili, W., Paasonen, P. H. M., Kulmala, M., Harriosn, R.M., Norford,
886 L., and Britter, R.: Ultrafine particles in cites, Environ. Intl., 66, 1-10, 2014.

887

888 Li, X. L., Wang, J. S., Tu, X. D., Liu, W., and Huang, Z.: Vertical variations of particle number
889 concentration and size distribution in a street canyon in Shanghai, China, Sci. Tot. Environ., 378,
890 306-316, 2007.

891

892 Lingard, J. J. N., Agus, E.L., Young, D. T., Andrew, G. E., and Tomlin, A. S.: Observations of
893 urban airborne particle number concentrations during rush-hour conditions: analysis of the number
894 based size distributions and modal parameters, J. Environ., Monitor., 8, 1203-1218, 2006.

895

896 Longley, I. D., Gallagher, M. W., Dorsey, J. R., Flynn, M., Allan, J. D., Alfarra, M. R., and Inglis,
897 D.: A case study of aerosol ($4.6\text{ nm} < D_p < 10\text{ }\mu\text{m}$) number and mass size distribution measurements
898 in a busy street canyon in Manchester, UK, Atmos. Environ., 37, 1563-1571, 2003.

899

900 Masiol, M., and Harrison, R. M.: Aircraft engine exhaust emissions and other airport-related
901 contributions to ambient air pollution: A review, Atmos. Environ., 95, 409-455, 2014.

902

903 Masiol, M., Harrison, R. M., Tuan, V. V., and Beddows, D. C. S.: Sources of sub-micrometre
904 particles near a major international airport, Atmos. Chem. Phys., 17, 12379-12403, 2017.

905

906 Morawska, L., Thomas, S., Bofinger, N., Wainwright, D., and Neale, D.: Comprehensive
907 characterization of aerosols in a subtropical urban atmosphere: Particle size distribution and
908 correlation with gaseous pollutants, Atmos. Environ., 32, 2467-2478, 1998.

909

910 Nikolova, I., Janssen, S., Vos, P., Vrancken, K., Mishra, V., and Berghmans, P.: Dispersion
911 modelling of traffic induced ultrafine particles in a street canyon in Antwerp, Belgium and
912 comparison with observations, Sci. Tot. Environ., 412, 336-343, 2011.

913

914 Nosko, O., Vanhanen, J., and Olofsson, U.: Emission of 1.3-10 nm airborne particles from brake
 915 materials, *Aerosol Sci. Technol.*, 51, 91-96, 2017.

916

917 NPL: Design, construction and testing of a humidity management system for ultrafine particle field
 918 measurements, National Physical Laboratory, NPL Report AS 48, 2010.

919

920 Oke, T., Mills, G., Christen, A., and Voogt, J.: *Urban Climates*, Cambridge University Press,
 921 doi:10.1017/9781139016476, 2017.

922

923 Olivares, G., Johansson, C., Strom, J., and Hansson, H.-C.: The role of ambient temperature for
 924 particle number concentrations in a street canyon, *Atmos. Environ.*, 41, 2145-2155, 2007.

925

926 Posser, L. N., and Pandis, S. N.: Sources of ultrafine particles in the Eastern United States, *Atmos.*
 927 *Environ.*, 111, 103-112, 2015.

928

929 Pushpawela, B., Jayaratne, R., and Morawska, L.: Differentiating between particle formation and
 930 growth events in an urban environment, *Atmos. Chem. Phys.*, 18, 11171-11183, 2018.

931

932 Rönkkö, T., Virtanen, A., Vaaraslahti, K., Keskinen, J., Pirjola, L., and Lappi, M.: Effect of
 933 dilution conditions and driving parameters on nucleation mode particles in diesel exhaust:
 934 Laboratory and on-road study, *Atmos. Environ.*, 40, 2893-2901, 2006.

935

936 Rönkkö, T., Kuuluvainen, H., Karjalainen, P., Keskinen, J., Hillamo, R., Niemi, J. V., Pirjola,
 937 L., Timonen, H. J., Saarikoski, S., Saukko, E., Järvinen, A., Silvennoinen, H., Rostedt, A., Olin,
 938 M., Yli-Ojanperä, J., Nousiainen, P., Kousa, A., and Dal Maso, M.: Traffic is a major source of
 939 atmospheric nanocluster aerosol, *PNAS*, 114, 7549-7554, 2017.

940

941 Salimi, F., Rahman, Md. M., Clifford, S., Ristovski, Z., and Morawska, L.: Nocturnal new particle
 942 formation events in urban environments, *Atmos. Chem. Phys.*, 17, 521-530, 2017.

943

944 Schneider, J., Hock, N., Weimer, S., Borrmann, S., Kirchner, U., Vogt, R., and Scheer, V.:
 945 Nucleation Particles in Diesel Exhaust: Composition Inferred from In Situ Mass Spectrometric
 946 Analysis, *Environ. Sci. Technol.*, 39, 6153-6161, 2005.

947

948 Shi, J. P., and Harrison, R. M.: Investigation of ultrafine particle formation during diesel exhaust
 949 dilution, *Environ. Sci. Technol.*, 33, 3730-3736, 1999.

950

951 Shi, J. P., Mark, D., and Harrison, R. M.: Characterization of Particles from a Current Technology
 952 Heavy-Duty Diesel Engine, *Environ. Sci. Technol.*, 34, 748-755, 2000.

953

954 Shi, J. P., Evans, D. E., Khan, A. A., and Harrison, R. M.: Sources and concentration of
 955 nanoparticles (< 10 nm diameter) in the urban atmosphere, *Atmos. Environ.*, 35, 1193-1202, 2001.

956

957 Timko, M. T., Fortner, E., Franklin J., Yu, Z., Wong, W., Onasch, T. B., Miake-Lye, R. C., and
 958 Herndon, S. C.: Atmospheric Measurements of the Physical Evolution of Aircraft Exhaust Plumes,
 959 *Environ. Sci. Technol.*, 2013, 47, 3513-3520, 2013.

960

961 Vakeva, M., Hameri, K., Kulmala, M., Lahdes, R., Ruuskanen, J., Laitinen, T.: Street level versus
 962 rooftop concentrations of submicron aerosol particles and gaseous pollutants in an urban street
 963 canyon, *Atmos. Environ.*, 33, 1385-1397, 1999.

964

- Van Dingenen, R., Raes, F., Putaud, J.-P., Baltensperger, U., Charron, A., Facchini, M.-C., Decesari, S., Fuzzi, S., Gehrig, R., Hansson, H.-C., Harrison, R. M., Hüglin, C., Jones, A. M., Laj, P., Lorbeer, G., Maenhaut, W., Palmgren, F., Querol, X., Rodriguez, S., Schneider, J., ten Brink, H., Tunved, P., Tørseth, K., Wehner, B., Weingartner, E., Wiedensohler, A., and Wåhlin, P.: A European aerosol phenomenology – 1: Physical characteristics of particulate matter at kerbside, urban, rural and background sites in Europe, *Atmos. Environ.*, 38, 2561-2577, 2004.
- Villa, T. F., Jayaratne, E. R., Gonzalez, L. F., and Morawska, L.: Determination of the vertical profile of particle number concentration adjacent to a motorway using an unmanned aerial vehicle, *Environ. Pollut.*, 230, 143-142, 2017.
- Vu, T. V., Delgado-Saborit, J. M., and Harrison, R. M.: Review: Particle number size distributions from seven major sources and implications for source apportionment studies, *Atmos. Environ.*, 122, 114-132, 2015a.
- Vu, T. V., Delgado-Saborit, J. M., Harrison, R. M.: A review of hygroscopic growth factors of submicron aerosols from different sources and its implication for calculation of lung deposition efficiency of ambient aerosol, *Air Qual. Atmos. Health*, doi 10.1007/s11869-015-0365-0, 2015b.
- Wang, Y., Hopke, P. K., Chalupa, D. C., and Utell, M. J.: Long-term study of urban ultrafine particles and other pollutants, *Atmos. Environ.*, 45, 7672-7680, 2011.
- Wehner, B., Birmili, W., Gnauk, T., and Wiedensohler, A.: Particle number size distributions in a street canyon and their transformation into the urban-air background: measurements and a simple model study, *Atmos. Environ.*, 36, 2215-2223, 2002.
- WHO: Air Quality Guidelines – Global Update 2005, World Health Organization, Copenhagen, 2006.
- WHO: Review of Evidence on Health Aspects of Air Pollution – REVIHAAP Project, World Health Organization, Copenhagen, 2013.
- Wiedensohler, A., Birmili, W., Nowak, A., Sonntag, A., Weinhold, K., Merkel, M., Wehner, B., Tuch, T., Pfeifer, S., Fiebig, M., Fjaraa, A.M., Asmi, E., Sellegri, K., Depuy, R., Venzac, H., Villani, P., Laj, P., Aalto, P., Ogren, J.A., Swietlicki, E., Williams, P., Roldin, P., Quincey, P., Hüglin, C., Fierz-Schmidhauser, R., Gysel, M., Weingartner, E., Riccobono, F., Santos, S., Gruning, C., Faloon, K., Beddows, D., Harrison, R.M., Monahan, C., Jennings, S.G., O'Dowd, C. D., Marinoni, A., Horn, H.-G., Keck, L., Jiang, J., Scheckman, J., McMurry, P. H., Deng, Z., Zhao, C. S., Moerman, M., Henzing, B., de Leeuw, G., Loschau, G., and Bastian, S.: Mobility particle size spectrometers: harmonization of technical standards and data structure to facilitate high quality long-term observations of atmospheric particle number size distributions, *Atmos. Meas. Tech.*, 5, 657-685, 2012.
- Wojdyr M.: Fityk: A General purpose peak fitting program, *J. Appl. Cryst.*, 43, 1126-1128, 2010.
- Zhu, Y., Hinds, W. C., Kim, S., and Sioutas, C.: Concentration and size distribution of ultrafine particles near a major highway, *JAWMA*, 52, 1032-1042, 2002a.
- Zhu, Y., Hinds, W. C., Kim, S., Shen, S., and Sioutas, C.: Study of ultrafine particles near a major highway with heavy-duty diesel traffic, *Atmos. Environ.*, 36, 4323-4335, 2002b.

1017 **TABLE LEGENDS**

1018

1019 **Table 1:** Location sites of instruments during the campaign. Mean sea level (msl), Above
1020 ground level (agl), Condensation particle counter (CPC), Scanning Mobility Particle
1021 Sizers (SMPS).

1022

1023

1024 **FIGURE LEGENDS**

1025

1026 **Figure 1:** Study area locations (a) in central London (UK) and (b) more detail of the Marylebone
1027 Road (MR), Westminster University (WU) and Regent's University (RU) sites.

1028

1029 **Figure 2:** Time series of total particle number count from the SMPS instruments at the five sites
1030 (Fig. 1, Table 1) over the campaign period.

1031

1032 **Figure 3:** Campaign-average diurnal variation of particle number counts derived from the SMPS
1033 instruments with median (line) and inter-quartile range (shading) shown.

1034

1035 **Figure 4:** Average particle number size distributions stratified by 45° wind directions sectors (°,
1036 measured at LHR, value indicates mid-point of sector) for (a) Marylebone Road, (b)
1037 North Kensington (c) Regent's University, (d) BT Tower.

1038

1039 **Figure 5:** Lognormal modes fitted to the average particle size spectrum at North Kensington
1040 for wind direction sector 270°.

1041 **Figure 6:** A schematic diagram of the wind flows in the street canyon of Marylebone Road (6
1042 traffic lanes) during southerly and northerly winds. The orange marker represents the
1043 MR sampling site and red marker represents the WM sampling site.

1044

1045 **Figure 7:** Time series (15 min) of ratio of total particle number counts, CPC/SMPS, for four
1046 sites over the campaign period.

1047

1048 **Figure 8:** Time series (15 min) of total particle number count from the CPC instruments located
1049 at four sites over the campaign period.

1050

1051 **Figure 9:** Time series (15 min) of (a) SMPS integrated counts, (b) particle number counts (CPC)
1052 and (c) Black Carbon from Marylebone Road, Westminster University and Regent's
1053 University for 30 January to 1 February 2017.

1054

1055

1056

1057 **Table 1:** Location sites of instruments during the campaign. Mean sea level (msl), Above ground level (agl), Condensation particle counter (CPC),
1058 Scanning Mobility Particle Sizers (SMPS).

1059

Site Name	Marylebone Road	Westminster University	Regent's University	BT Tower	North Kensington
Lat (° N), Long (°W)	51.522530, 0.154611	51.522322.0.15515	51.525542, 0.154570	51.521426, 0.138924	51.521082, 0.213403
Height of ground msl (m)	26	26	30	25	23
Height of inlets agl (m)	4	26	17	160	3
Instruments installed	Long_DMA_SMPS/ CPC Vaisala CL31	Long_DMA_SMPS/CPC/ (Micro)Aethalometer/Anemometer	Long_DMA_SMPS/ Short_DMA_SMPS/ CPC/Aethalometer/Anemometer	Long_DMA_SMPS/CPC/ (Micro) Aethalometer/Anemometer	Long_DMA_SMPS Vaisala CL31
Particle spectrometer type	3080+3081+3775	3080+3081+3776	(3082+3081+3775)/(3082+3085+3776)	(3080+3081+3775)	(3080+3081+3775)
Aerosol dryer	Yes	No	No	No	Yes
CPC type	TSI 3025	TSI 3776	TSI 3776	TSI 3775	None

1060

1061 Note: The SMPS size ranges are given in Section 2.2. The lower size cuts (D_{50}) of the CPCs are 3 nm (3025), 2.5 nm (3776) and 4 nm (3775).

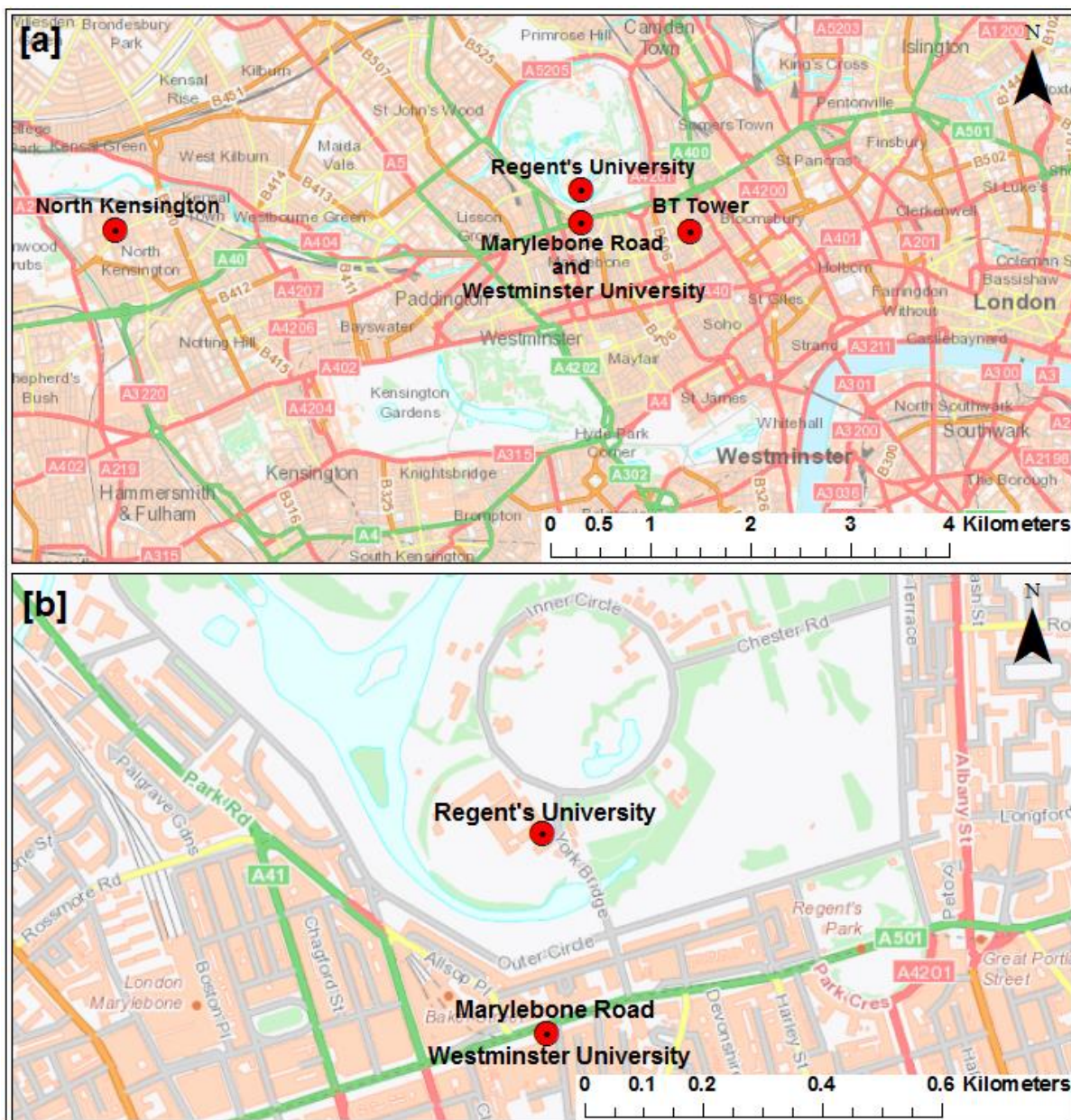
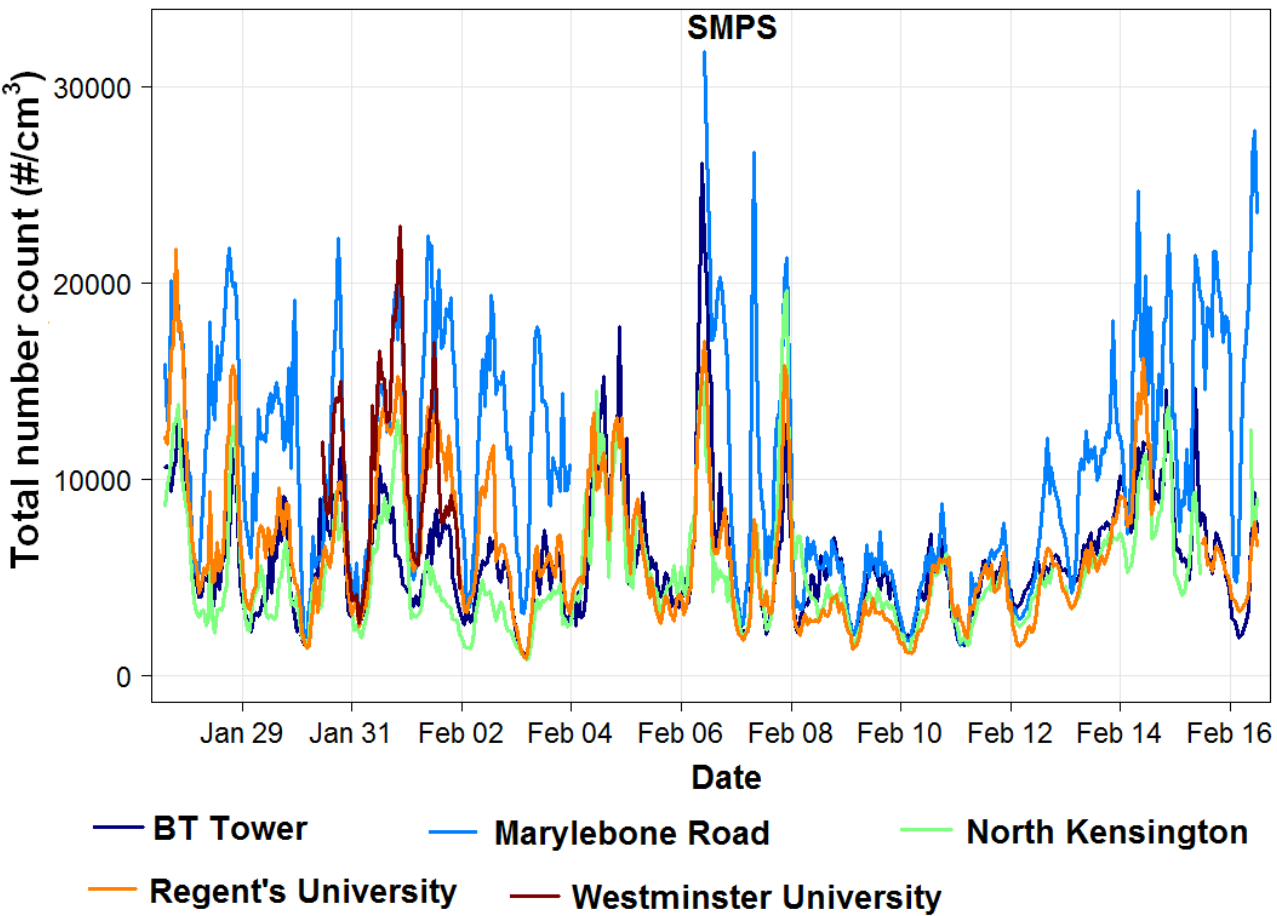


Figure 1: Study area locations (a) in central London (UK) and (b) more detail of the Marylebone Road (MR), Westminster University (WU) and Regent's University (RU) sites.

1067



1068

1069

1070

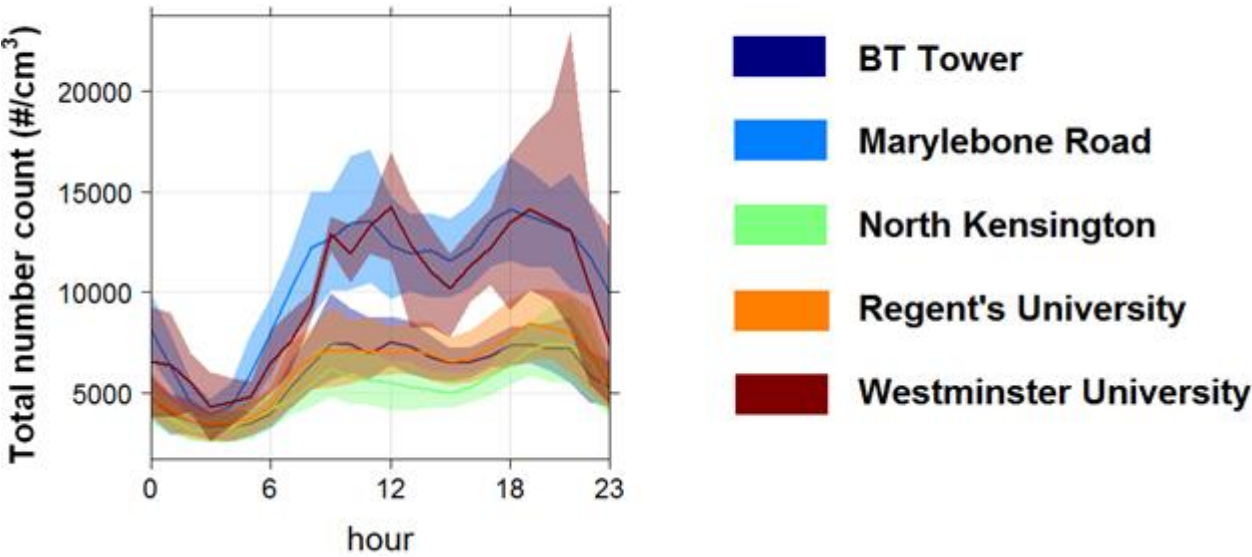
1071

1072

1073

Figure 2: Time series of total particle number count from the SMPS instruments at the five sites (Fig. 1, Table 1) over the campaign period.

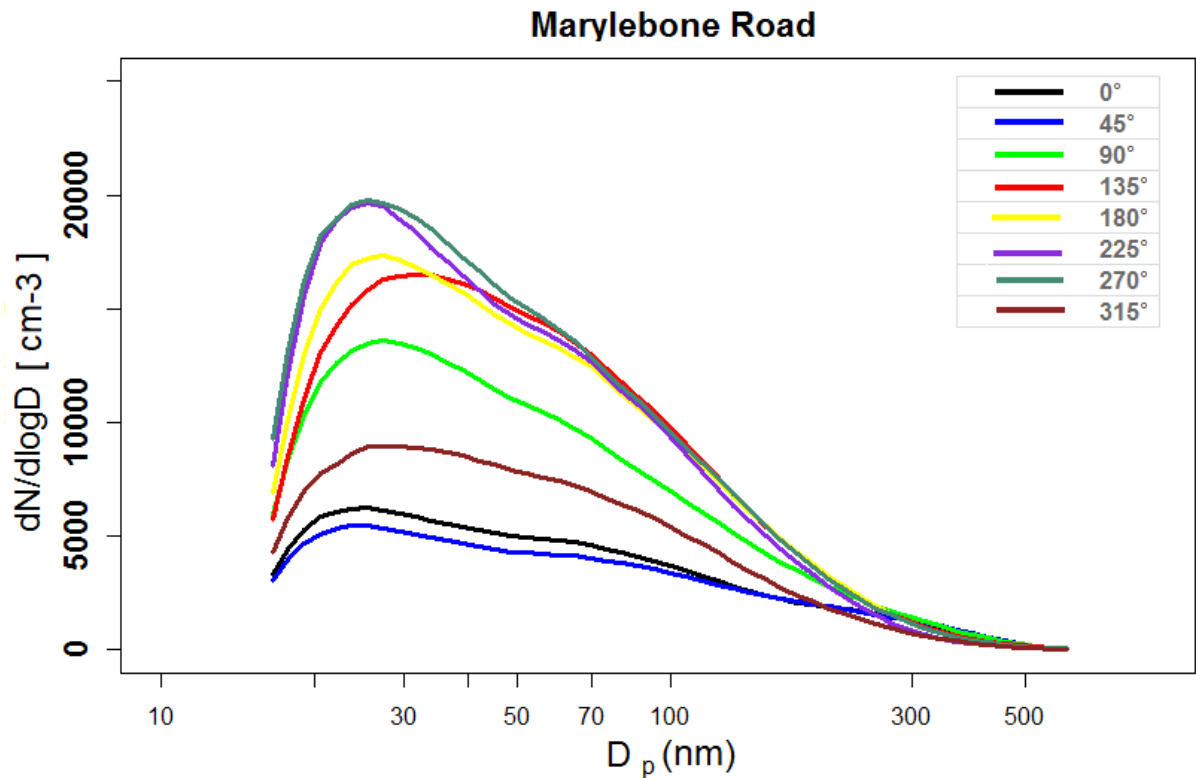
1074
1075
1076



1077
1078
1079
1080
1081
1082
1083
1084
1085
1086

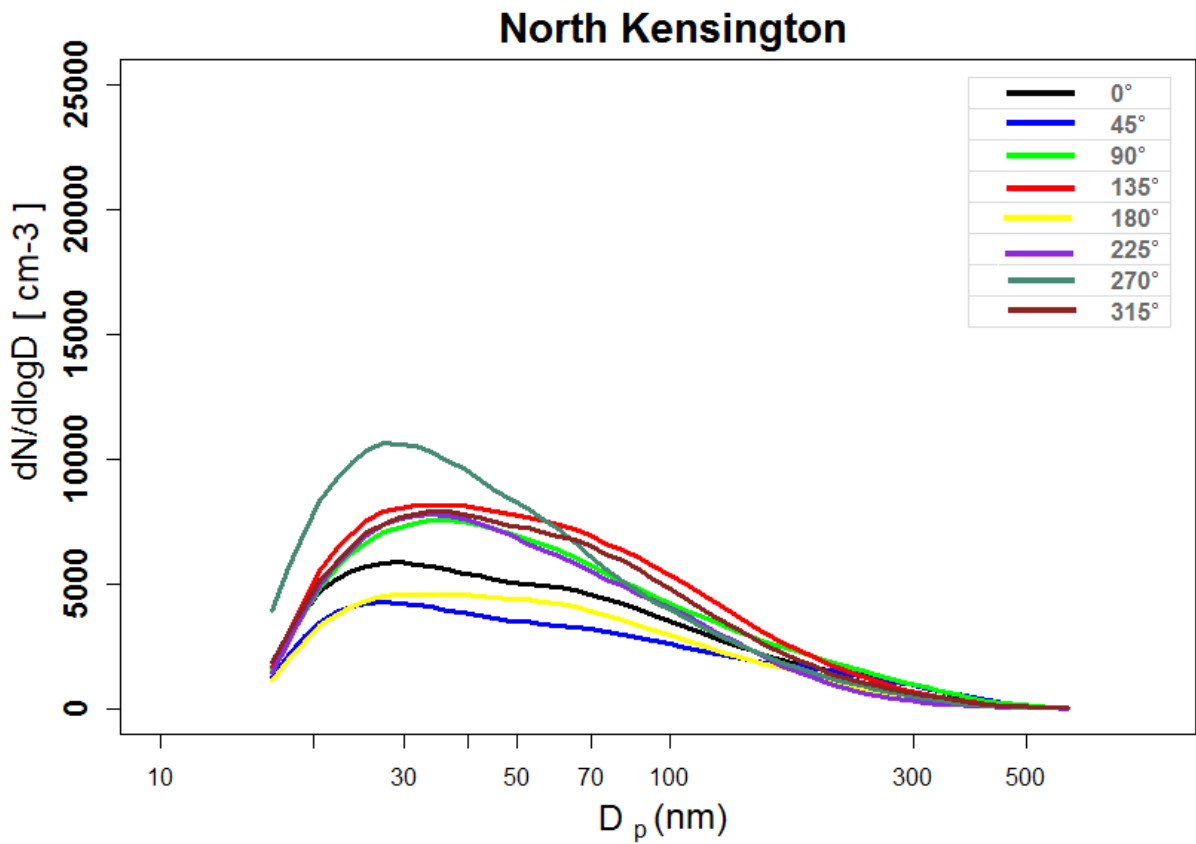
Figure 3: Campaign-average diurnal variation of particle number counts derived from the SMPS instruments with median (line) and inter-quartile range (shading) shown.

(a)



1087

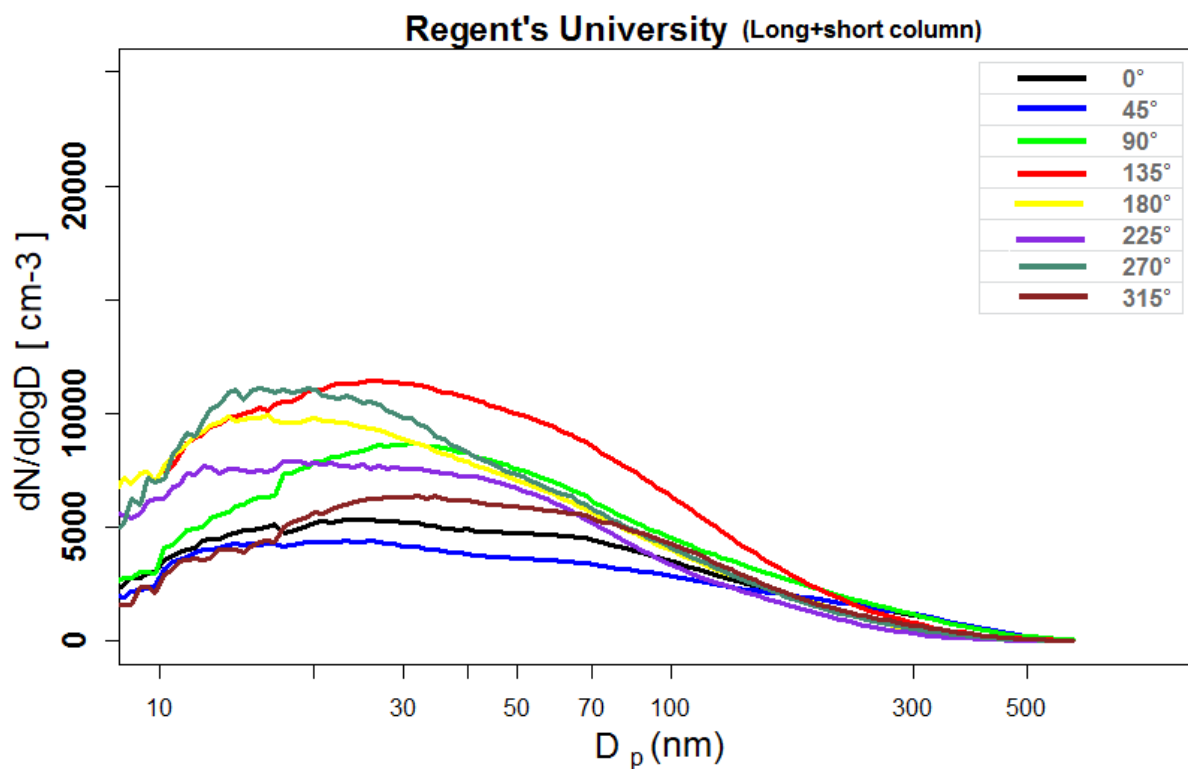
(b)



1089

1090

(c)



(d)

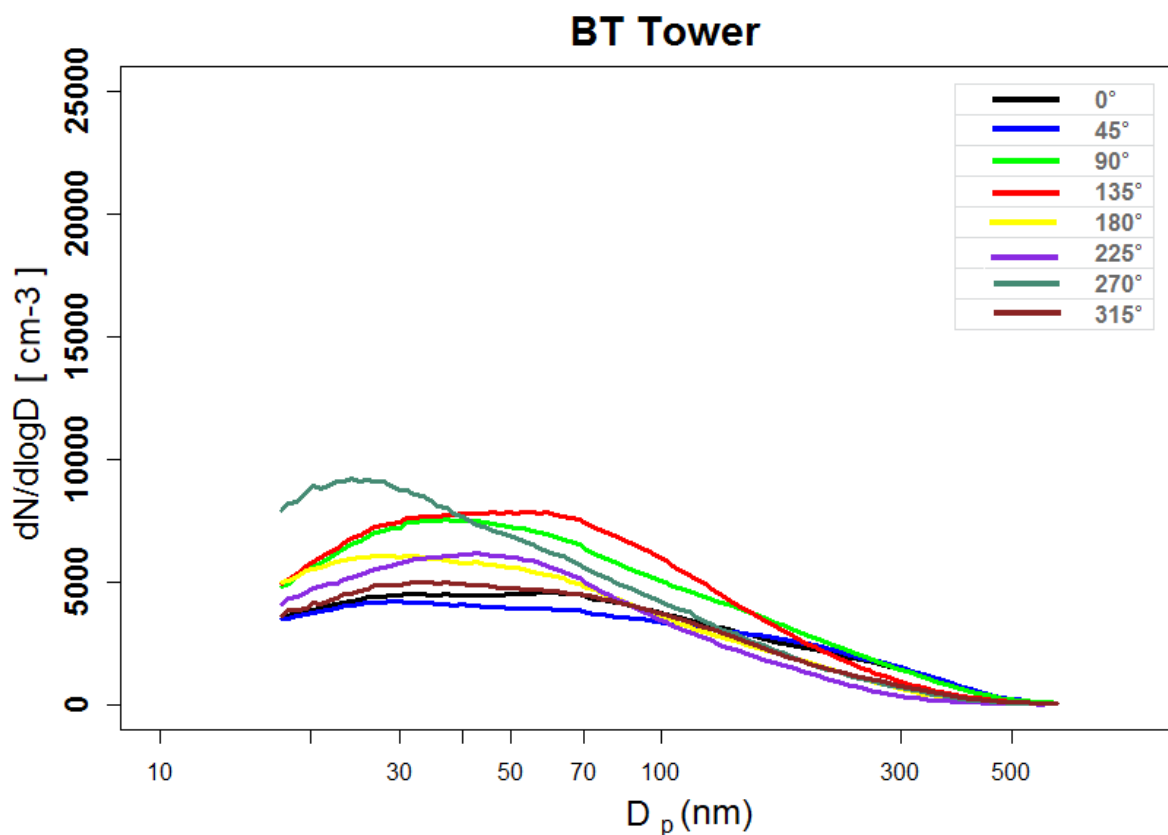
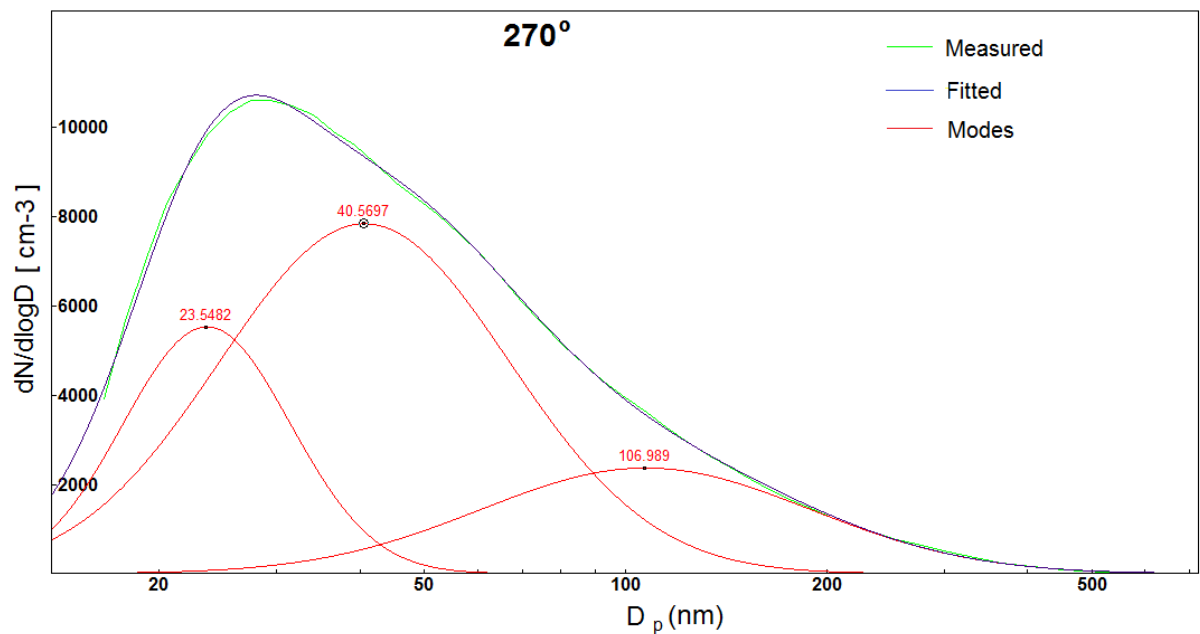


Figure 4: Average particle number size distributions stratified by 45° wind directions sectors (°, measured at LHR, value indicates mid-point of sector) for (a) Marylebone Road, (b) North Kensington (c) Regent's University, (d) BT Tower.

1098



1099

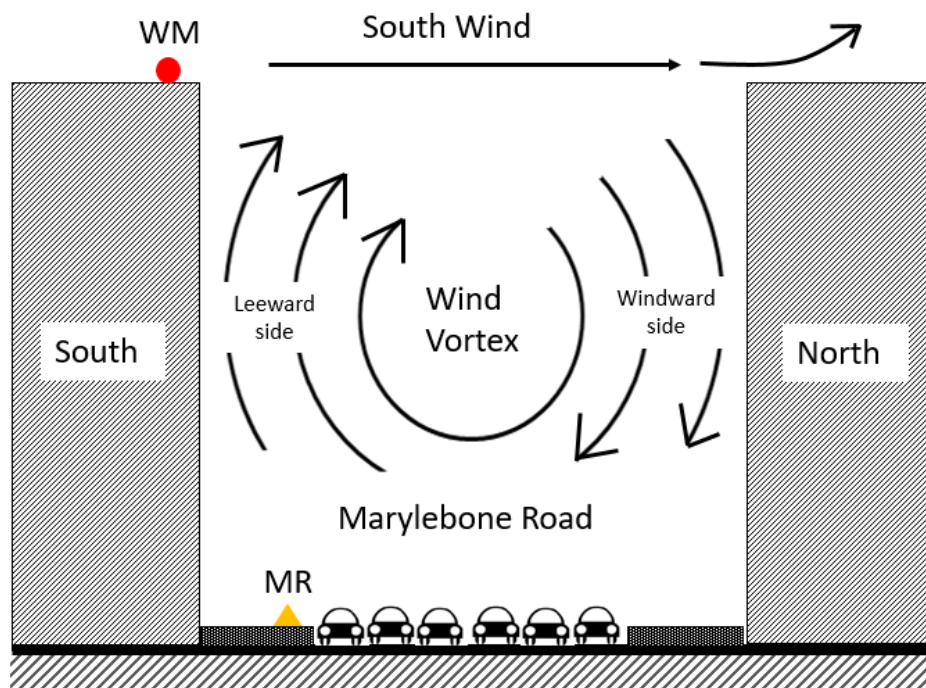
1100

1101

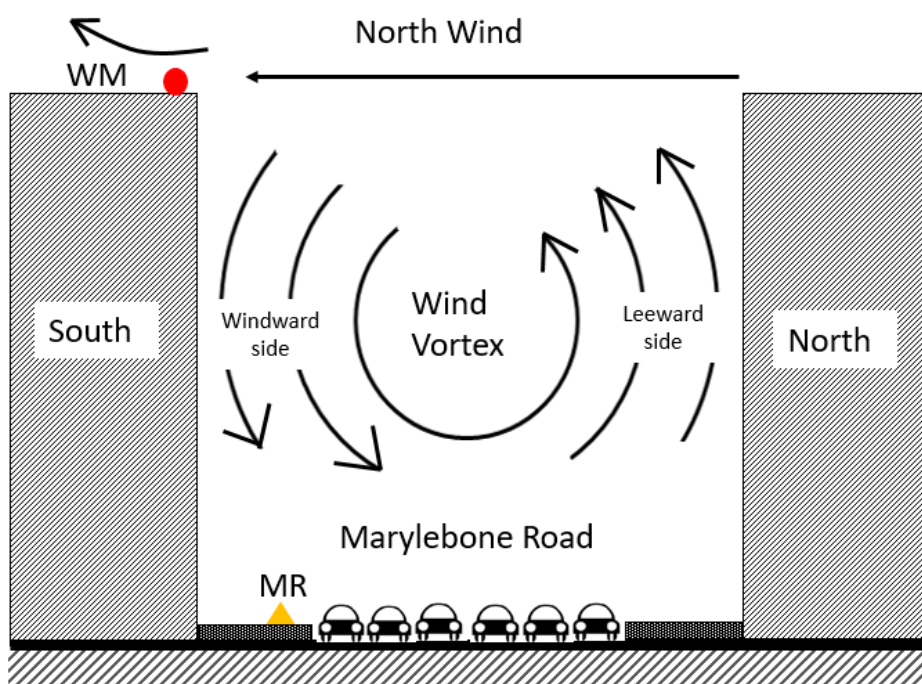
1102

1103

Figure 5: Lognormal modes fitted to the average particle size spectrum at North Kensington for wind direction sector 270°.



1104



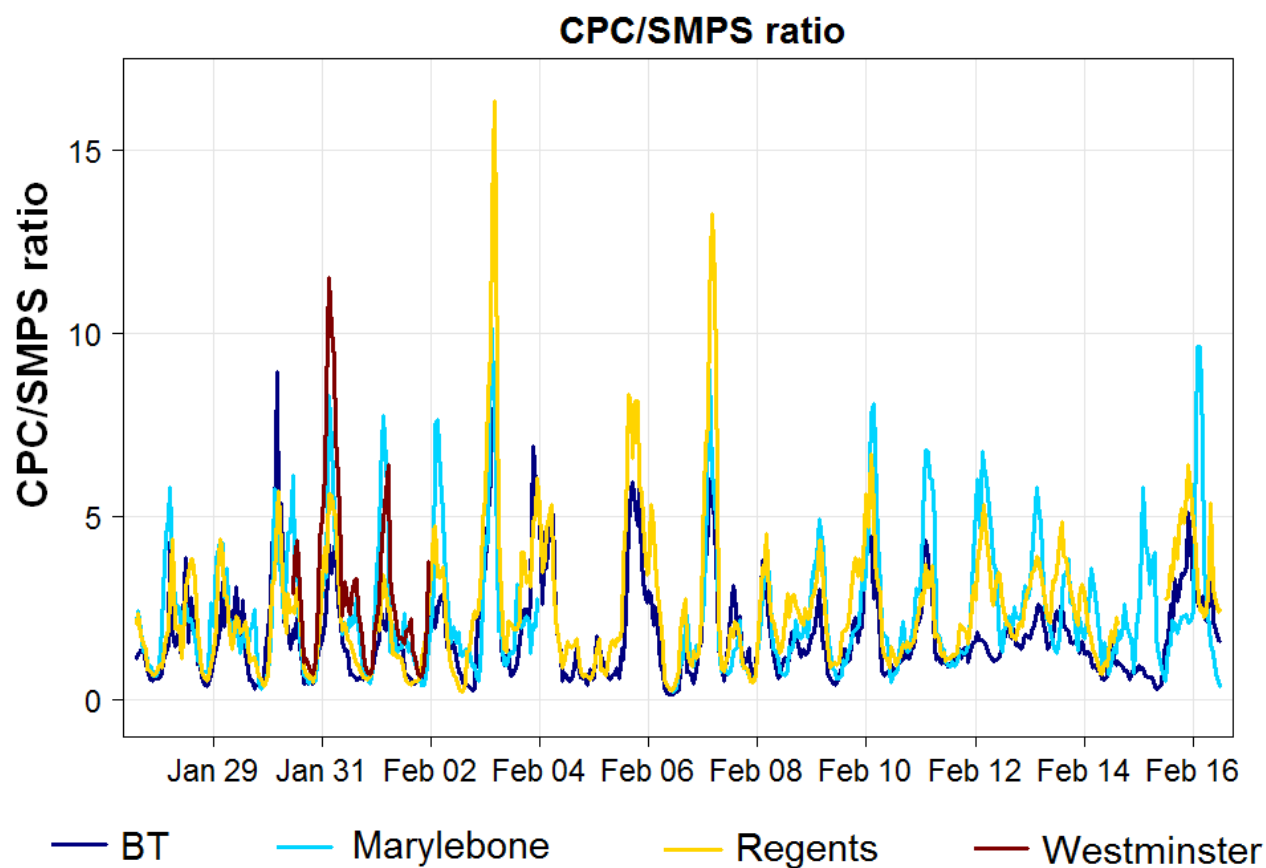
1105

1106 **Figure 6:** A schematic diagram of the wind flows in the street canyon of Marylebone Road (6
 1107 traffic lanes) during southerly and northerly winds. The orange marker represents the MR sampling
 1108 site and red marker represents the WM sampling site.

1109

1110

1111
1112

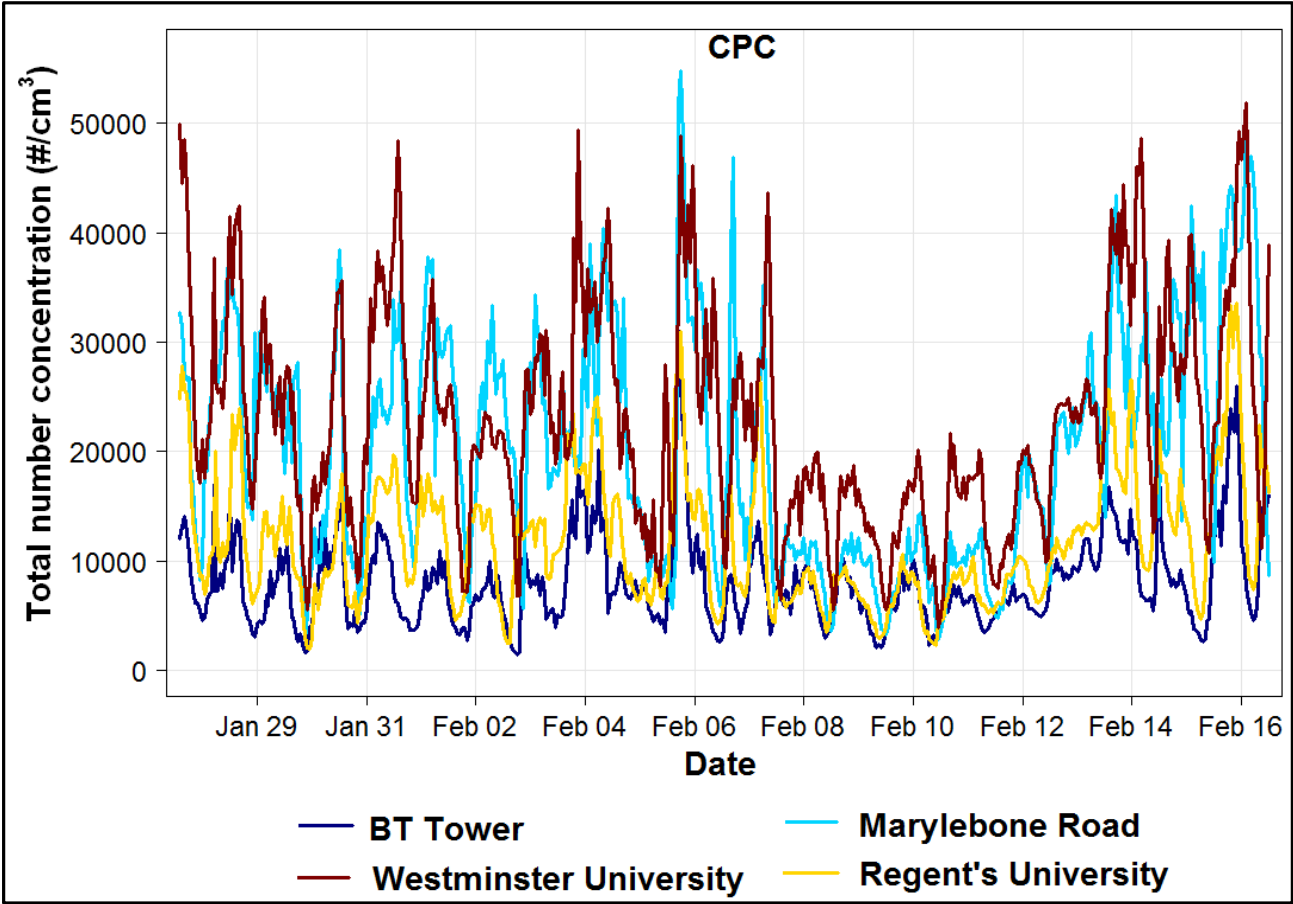


1113
1114
1115
1116
1117

Figure 7: Time series (15 min) of ratio of total particle number counts, CPC/SMPS, for four sites over the campaign period.

1118
1119
1120
1121
1122
1123
1124
1125
1126
1127
1128
1129
1130

1131



1132

1133

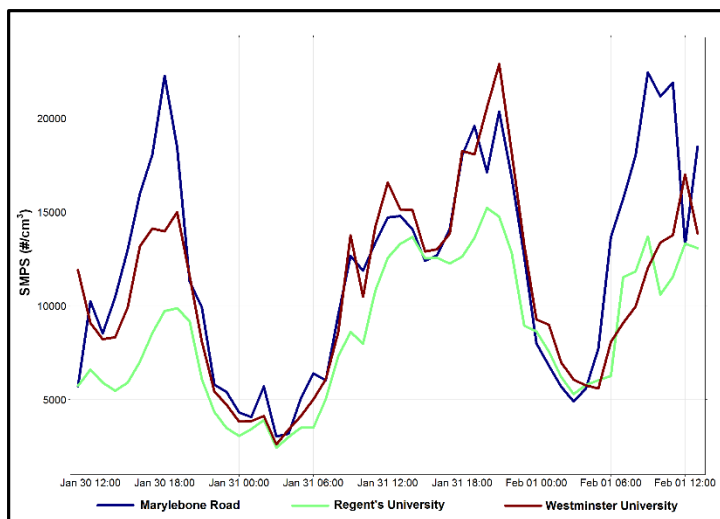
1134

1135

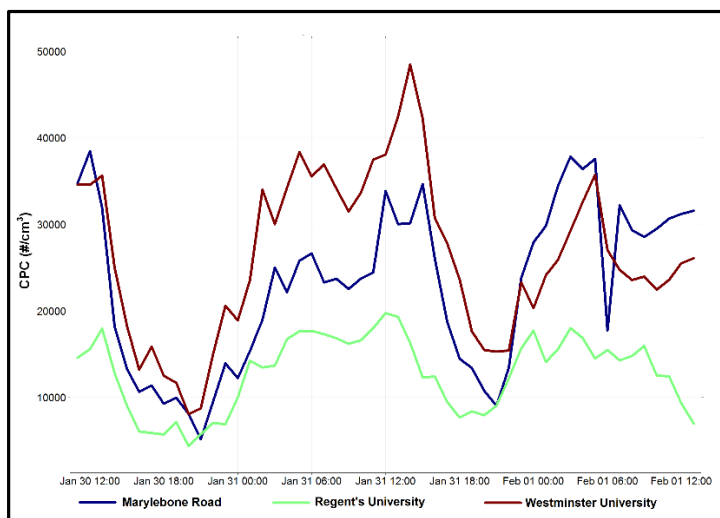
1136

1137

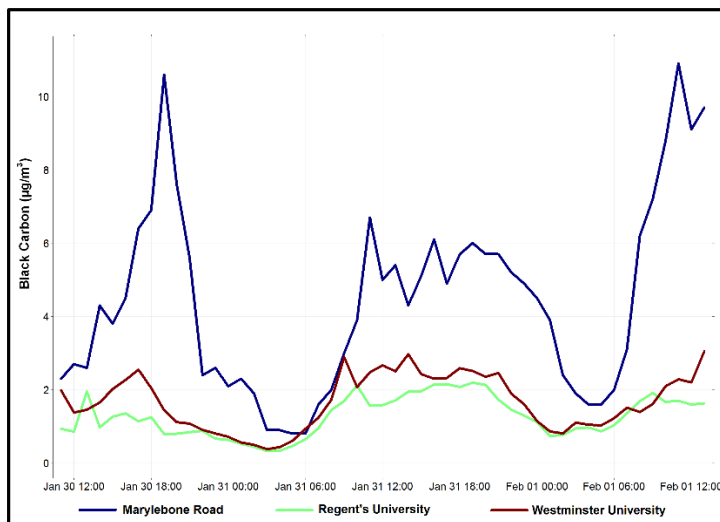
Figure 8: Time series (15 min) of total particle number count from the CPC instruments located at four sites over the campaign period.



1138
(a)



(b)



1142
(c)

Figure 9: Time series (15 min) of (a) SMPS integrated counts, (b) particle number counts (CPC) and (c) Black Carbon from Marylebone Road, Westminster University and Regent's University for 30 January to 1 February 2017.